VIBRATIONAL AND CHEMICAL NONEQUILIBRIUM IN A STOICHIOMETRIC TURBOJET ENGINE USING KEROSINE-TYPE FUEL

Wiley Paul DeCarli

NAVAL POSTGRADUATE SCHOOL
Monterey, California

THESIS

VIBRATIONAL AND CHEMICAL NONEQUILIBRIUM IN A STOICHIOMETRIC TURBOJET ENGINE USING KEROSINE-TYPE FUEL

by

Wiley Paul DeCarli

Thesis Advisor: Dr. A. E. Fuhs

March 1972

Vibrational and Chemical Nonequilibrium in a Stoichiometric Turbojet Engine Using Kerosine-Type Fuel

by

Wiley Paul DeCarli
Lieutenant Commander, United States Navy
B.S., University of Idaho, 1963

Submitted in partial fulfillment of the
requirements for the degree of

MASTER OF SCIENCE IN AERONAUTICAL ENGINEERING

from the

NAVAL POSTGRADUATE SCHOOL
March 1972

ABSTRACT

The effects of vibrational and chemical nonequilibrium on turbine performance were investigated separately. The vibrational model was taken as a pure nitrogen expansion, and the chemical model was taken as the combustion products of a stoichiometric mixture of kerosine and air. The loss of performance of fully frozen flow with respect to the equilibrium flow for each model was determined. The extent to which nonequilibrium will occur was investigated within limited ranges of pressure and temperature. Vibrational nonequilibrium can result in losses up to seven percent with respect to equilibrium flow. Vibrational freezing will be virtually complete a short distance after the throat of the first stator assembly. The losses due to chemical nonequilibrium are insignificant compared to the vibrational nonequilibrium losses.

TABLE OF CONTENTS

LIST OF TABLES

LIST OF ILLUSTRATIONS

Figure Page

TABLE OF SYMBOLS AND ABBREVIATIONS

A/A^*	Ratio of local area to throat area
C_p	Specific heat capacity at constant pressure
E_v	Total vibrational energy
$E_v{}^*$	Total equilibrium vibrational energy
$E_{v_{th}}{}^*$	Total equilibrium vibrational energy at the stator throat
h	Static enthalpy
H	Total enthalpy
$\Delta H^\circ{}_{f_i}$	Enthalpy of formation of specie i at reference pressure and temperature
m_i	Molecular weight of specie i
M	Mach number
$\overline{M}$	Molecular weight of gas mixture
P	Pressure
Q_r	Energy added to the rotational-translational gas
Q_D	Difference in vibrational energy between stations one and three
$\overline{R}$	Gas constant
$S(T, P)$	Entropy at temperature T and pressure P
T	Temperature
U	Velocity
x	Distance along midspan streamline
X	Mole fraction
Y	Mass fraction
γ	Ratio of specific heat capacities
η_c	Chemical efficiency

η_v	Vibrational efficiency
τ	Relaxation time

Subscripts

v	Vibrational
R	Rotational
T	Translational
t	Total or stagnation conditions
o	Reference conditions

ACKNOWLEDGEMENT

The author wishes to acknowledge the guidance and consultation of Dr. A. E. Fuhs of the Aeronautics Department of the Naval Postgraduate School in his capacity as thesis advisor.

Acknowledgement is also extended to Dr. D. W. Netzer for his timely guidance.

I. INTRODUCTION

The aircraft of tomorrow must be capable of operating at high Mach number, have large amounts of excess thrust, be capable of operating at high altitude, and yet be very economical. As the requirement for these aircraft becomes more prevalent, designers of both airframes and power plants must strive to match their respective ideas to produce a viable design. The airframe specialist is concerned with drag and high skin-temperature problems which he hopes to resolve by reduction of frontal area and by lighter gross weights. The power plant specialist investigates higher turbine inlet temperatures because of the increased efficiency of the cycle with high peak temperatures. The increase in flight Mach number induces a rise in the temperature of the cooling air available at the turbine. This higher temperature reduces the cooling potential of the air.

The next generations of the turbojet engine will utilize nearly double the present turbine inlet temperature by burning stoichiometrically. As the turbine inlet temperature is increased, the effects of dissociation and vibrational excitation play a significant role in the energy balance. The jump in turbine temperature for stoichiometric combustion will produce almost triple the degree of vibrational excitation, a large increase in local velocities for the same local Mach number within the engine, and a substantial rise in the degree of dissociation of the products of combustion.

The phenomenon of vibrational energy freezing occurs due to the relatively large number of molecular collisions required to return the vibrational mode of internal energy to equilibrium. Freezing of chemical composition occurs when the gas cannot react fast enough to maintain equilibrium with a rapidly changing temperature and pressure. Both of these phenomena are familiar to the rocket designer. The relatively low temperatures and high pressures characteristic to the turbojet cycle in the past have not caused these nonequilibrium effects to any significant degree.

The presence of nonequilibrium in the form of frozen vibrational energy and/or frozen chemical composition is very probable in the turbine section of an advanced high temperature turbojet. The rapid removal of work from the gas in the turbine reduces both the temperature and pressure at a rapid rate. The vibrational temperature is the independent variable in the vibrational energy distribution, and there is a corresponding temperature for both rotation and translation. At equilibrium, the rotation, translation, and vibration temperatures are the same. Comparison of the vibrational, rotational, and translational temperatures in the turbine would show a more rapid decrease in the latter two relative to the rate of vibrational temperature decrease, primarily due to the number of collisions required to maintain equilibrium. The magnitude of the relaxation time relative to the short transit time in the turbine suggests that a significant degree of vibrational freezing may result. The effect of lower pressure would be to

reduce the collision frequency, thereby increasing the relaxation times.

Evaluation of the loss of available energy due to vibrational freezing becomes rather complicated in multicomponent gases and involves complex-numerical computer programs. Stollery and Park [17] and Wilson, et al. [22] give examples of these programs. Exact calculations of recombination and dissociation rates of a mixture of gases such as combustion products also involve complex computer programs. The complexity of the entire problem is a result of the number of nonlinear equations involved and the lack of an exact solution to the flow problem in rotating machines.

This thesis attempts to apply the nonequilibrium analysis of vibrational and chemical freezing to the turbine section of a turbojet cycle. The presence and degree of each of these problems are investigated, and the effects of changing the thermodynamic parameters of the cycle are discussed.

II. ANALYSIS

High velocity flows frequently create rapid changes in the flow variables: temperature, pressure, and density. The internal modes of freedom of the gas molecules do not always remain in equilibrium or return to equilibrium fast enough to keep pace with the rapidly changing macroscopic environment. The return to equilibrium of these internal modes is governed by internal kinetic equations. The existence of chemical reactions in the flow introduces the chemical kinetic equations. There are characteristic times associated with each of these processes: relaxation time with the internal kinetic equations and reaction times with the chemical kinetic equations.

Maintenance of equilibrium of chemical reaction and of internal degrees of freedom requires a number of molecular collisions. It is obvious that true equilibrium flow cannot exist. The average time for a unit mass of gas to transit a turbine is a prime factor in determining whether or not freezing occurs. The conversion of available energy to useful work by the turbine is accomplished in a small distance, and present turbine technology involves Mach numbers in the transonic range. These facts, combined with high local temperatures, produce a local fluid velocity relative to the blade of the order of two to three thousand feet per second. The short physical length of the turbine results in an extremely low transit time. If the characteristic times of

progression of the chemical and molecular phenomena are very small compared to the time intervals of interest in the flow, the flow may be considered to be in local equilibrium. Conversely, if these characteristic times are much larger than the time intervals of interest in the flow, the phenomena may be considered frozen.

Theoretical description of a nonequilibrium flow requires incorporation of the kinetic equations describing the processes into the usual gas-dynamic conservation equations. Analysis and solution of such systems of equations are difficult; in all but the simplest problems, numerical methods are required. Bray and Appleton [5] and Anderson, et al. [2], have presented detailed analytical solutions to these problems.

Extensive research into nonequilibrium flows was inspired by the advent of space exploration. The flow around re-entry vehicles at high altitudes involves complex nonequilibrium chemistry [6]. In rocket propulsion systems, the problems of large expansion ratios and low exit pressures tended to magnify the situation. Excellent literature surveys by Read [15], Rich and Treanor [16], and Taylor and Bitterman [18] provide a myriad of data on vibrational relaxation. Gas dynamic lasers employ intentional vibrational nonequilibrium to obtain population inversions [3].

The complexity of solution of the expansion of combustion products through a turbine should be readily apparent. The problem must therefore be simplified in order to obtain meaningful conclusions as to the effects of nonequilibrium phenomena on the expansion. The interaction of vibrational

excitation and chemical reaction is not solved here, but some insight into the level of existence of each phenomenon is presented.

The effects and mechanics of vibrational nonequilibrium flow are considered separately from the effects and mechanics of chemical nonequilibrium flow.

A. VIBRATIONAL NONEQUILIBRIUM FLOW

In order to investigate the effects of vibrational nonequilibrium in a turbine, a simplified model was utilized. The expansion of pure gaseous nitrogen through a turbine was considered instead of the more complex case of the actual combustion products. Nitrogen was a good model for a number of reasons. By using a pure gas, no chemical reaction, other than dissociation, was present. The degree of dissociation in the temperature range considered was negligible. The problem of vibrational freezing could therefore be isolated, and the calculation of thermodynamic data for the flow was greatly simplified. In addition, the mole fraction of nitrogen is large in the gas mixture.

The following assumptions were expeditious:

1. Complete (microscopic and macroscopic) equilibrium existed at the exit of the combustion chamber.
2. The gas behaved as an ideal, inviscid fluid.
3. The turbine expansion was adiabatic.
4. The flow was considered as quasi one-dimensional.
5. The velocity of the gas at the combustion chamber outlet was considered negligible compared to the gas velocity after the turbine exit.

A turbine schematic (Figure 1) was defined. At station one, corresponding to burner outlet, the nitrogen was considered to be in complete equilibrium. Between stations one and two, the gas was expanded isentropically through the turbine. The work extracted by the turbine was assumed to be drawn strictly from the translational and rotational modes of internal energy. These modes were considered to be in equilibrium with each other during the entire process due to the relatively small number of collisions required for equilibrium. This model assumes the independence of the separate modes of internal energy. The validity of this procedure may not be universal in its application but was utilized here for simplicity of analysis. The vibrational energy was considered frozen in this expansion process. (See Figure 2.)

Between station two and station three, the gas was allowed to return to complete equilibrium in a constant area duct. This was accomplished by the redistribution of excess vibrational energy to the rotational-transational gas through a process equivalent to Rayleigh heating. The rotational and translational modes were considered to be always in complete equilibrium.

The extraction of work results in a decrease of total enthalpy. A hypothetical stagnation temperature of the rotational-translational gas at station two, T'_{t_2}, was chosen to represent a given amount of work extracted by the turbine. The prime represents the state of the rotational-translational gas. The ratio of specific heats, γ, was taken as a constant

and equal to that obtained by classical equipartition concepts for a diatomic gas with only rotational and translational modes. This value is $\gamma = 1.4$. The selection of a burner outlet stagnation pressure and temperature and a Mach number at station two, based on the chosen rotational-translational (RT) gas temperature, enabled the determination of the station two stagnation pressure through the use of the ideal gas isentropic relationship in equation (1).

$$P'_{t_2} = P_{t_1} \left[\frac{T'_{t_2}}{T_{t_1}} \right]^{\frac{\gamma}{\gamma-1}} \tag{1}$$

Use of an isentropic procedure is consistent with the desire to isolate vibrational nonequilibrium.

Downstream of station two, the gas was subjected to a Rayleigh heating process due to the relaxation of the vibrational mode.

$$Q_r + C_{P_{RT}} T'_2 + \frac{U_2^2}{2g} = C_{P_{RT}} T'_3 + \frac{U_3^2}{2g} \tag{2}$$

Utilizing the definition of stagnation enthalpy,

$$Q_r + H'_2 = H'_3 \tag{3}$$

where Q_r represents the energy added to the RT gas from the vibrational mode.

Equation (3) may be rewritten as:

$$Q_r = H'_3 - H'_2 = C_{P_{RT}} (T'_{t_3} - T'_{t_2}) \tag{4}$$

The ideal gas isentropic relationship was used to find static temperature, T'_2, which was needed in the iteration procedure.

$$T'_2 = \frac{T'_{t_2}}{1 + \frac{\gamma - 1}{2} M_2'^{2}} \qquad (5)$$

The determination of the Mach number at point three was then required. This value was determined by an iterative process matching the Rayleigh heat added to the classic definition of enthalpy. The enthalpy was considered as

$$h(T) = \int_{T_o}^{T} C_P \, dT \qquad (6)$$

Since the internal energy modes were considered separable, the specific heat may be expressed as

$$C_P = C_{P_R} + C_{P_T} + C_{P_V} = C_{P_{RT}} + C_{P_V} \qquad (7)$$

Using equation (7), equation (6) may be expressed as

$$h(T) = \int_{T_o}^{T} C_{P_{RT}} \, dT + \int_{T_o}^{T} C_{P_V} \, dT \qquad (8)$$

The energy added to the equilibrium RT gas in the Rayleigh heating model must be identically equal to the difference in the vibrational energy of the complete gas between stations one and three. This difference was taken thusly

$$h(T_1) = \int_{T_o}^{T_1} C_{P_V} \, dT + \int_{T_o}^{T_1} C_{P_{RT}} \, dT \qquad (9)$$

Therefore

$$h(T_1) = \int_{T_o}^{T_1} C_{P_V} \, dT + C_{P_{RT}} (T_1 - T_o)$$

Similarly

$$h(T_3) = \int_{T_o}^{T_3} C_{P_V}\, dT + C_{P_{RT}} (T_3 - T_o) \qquad (10)$$

Taking the difference between equations (9) and (10)

$$h(T_1) - h(T_3) = \int_{T_3}^{T_1} C_{P_V}\, dT + C_{P_{RT}} (T_1 - T_3) \qquad (11)$$

Now define, Q_D, as the difference in the vibrational energy between stations two and three.

$$Q_D = \int_{T_3}^{T_1} C_{P_V}\, dT \qquad (12)$$

Substituting equations (11) into equation (12)

$$Q_D = h(T_1) - h(T_3) - C_{P_{RT}} (T_1 - T_3) \qquad (13)$$

The iteration was satisfied when Q_r of equation (4) was equal to Q_D of equation (12). The actual solution for a given set of input parameters was obtained by entering gas tables [11] with the chosen M_2'. With the already chosen value of T_{t_2}', the values of T_t^* and T^* were obtained. A Mach number at station 3' was assumed, and equation (4) was solved in the following form,

$$Q_r = T_t^* \, C_{P_{RT}} \left[\frac{T_{t_3}'}{T_t^*} - \frac{T_{t_2}'}{T_t^*} \right] \qquad (14)$$

Utilizing information from gas tables [11] the temperature, T_3', was also obtained and equation (12) was evaluated. This process was repeated until Q_r and Q_D were within 0.5% of each

other. Satisfaction of the iteration process allowed calculation of stagnation temperature and pressure at station three.

The investigation of performance lost due to vibrational freezing required a reference quantity. This reference quantity was taken as the turbine work produced by the expansion of the gas with full equilibrium between the modes of vibration, rotation, and translation. For both equilibrium and nonequilibrium cases, the turbine pressure ratios were assumed identical.

Efficiency was defined as the ratio of actual work to ideal work where the actual work was considered as the work obtained from the vibrationally frozen model and the ideal work as that obtained from an equilibrium gas expanding to the same stagnation pressure.

$$\eta_v = \frac{\text{vibrationally frozen work}}{\text{equilibrium work}} \tag{15}$$

$$\eta_v = \frac{H(T_{t_1}) - H(T_{t_3})}{H(T_{t_1}) - H(T^*_{t_3})} \tag{16}$$

where $T^*_{t_3}$ is the ideal stagnation temperature at the stagnation pressure of station three.

The stagnation temperature for an ideal turbine evaluated at the stagnation pressure of station three was determined by isentropic relationships. By definition,

$$S(T_{t_1}, P_{t_1}) = S(T^*_{t_3}, P^*_{t_3}) \tag{17}$$

and

$$S(T, P) = S^\circ(T) - \bar{R}\,\ell n\,(P) \tag{18}$$

where S°(T) is the entropy of the gas at a given temperature and a pressure of one atmosphere. Using equation (18) in equation (17)

$$S^\circ(T_{t_1}) - \bar{R}\,\ln P_{t_1} = S^\circ(T^*_{t_3}) - \bar{R}\,\ln P^*_{t_3} \qquad (19)$$

It was chosen that $P^*_{t_3} = P'_{t_3}$ and the values of T_{t_1} and P_{t_1} were assumed. Therefore, an equation for the entropy at the desired temperature was obtained.

$$S^\circ(T^*_{t_3}) = S^\circ(T_{t_1}) + \bar{R}\,\ln\left[\frac{P^*_{t_3}}{P_{t_1}}\right] \qquad (20)$$

Solution of this equation yielded $T^*_{t_3}$ which was utilized to compute values of efficiency from equation (16). This efficiency represents a loss of performance resulting from non-equilibrium flow.

A method to identify the significance of vibrational non-equilibrium had been established, and the question of actual presence of this phenomenon in a high temperature turbine remained.

The complexity of the problem of vibrational relaxation precludes actual solution of the theoretical equations within the scope of this thesis, and experimental results of other researchers will be utilized in the ultimate discussion of the effects of this phenomenon on turbine flow. For complete understanding it is prudent, however, to develop the principles involved.

The nitrogen gas was considered to be a system of harmonic oscillators. This system of diatomic molecules was assumed to be capable of collisional interchange of energy with the

translational and rotational degrees of freedom of a heat bath at temperature T. The heat bath was provided by the translational and rotational degrees of freedom of the pure gas. At equilibrium, the distribution of oscillators over the energy states was assumed to be given by the Boltzmann distribution.

The majority of data on vibrational nonequilibrium, both theoretical and experimental, has been developed for the lag of vibrational equilibrium when vibrational degrees of freedom are being excited. Rich and Treanor [16] point out that there is evidence that the relaxation time for de-exitation may be one-fifth or smaller relative to the exitation relaxation time. The relaxation time is a measure of the rate of return to equilibrium after a disturbance.

The equation for the time rate of change of the number of molecules in a particular energy state may be developed using statistical thermodynamics and quantum mechanics. The rate of transition from one state to another is dependent upon the number of collisions per unit time between the oscillators and the molecules of the heat bath that possess sufficient energy to cause transition and on the probability that a single collision will result in transition.

For gas dynamic purposes the total vibrational energy is more useful than the molecular energy level population in each energy level. This total energy is a summation over all possible levels of the product of the energy in a particular level and the number of molecules in that level. Manipulation

of the rate of change of the molecular level population equation produces an equation for the rate of change of total vibrational energy. Vincenti and Kruger [20] express this as

$$\frac{dE_v}{dt} = \frac{E_v^* - E_v}{\tau} \tag{21}$$

where E_v is total vibrational energy, E_v^* is total vibrational energy at equilibrium, and τ is the relaxation time.

This equation shows that the vibrational energy of the system will always move toward equilibrium and that the rate of this movement at any instant is linearly related to the degree of departure from equilibrium at that instant. Even though this equation assumed a Boltzmann distribution only at equilibrium and no restriction is placed on the amount of departure of vibrational energy from equilibrium, Vincenti and Kruger [20] limit the equation to small departures from equilibrium. The limitation to small departures is a result of the anharmonicity of actual molecules.

The relaxation time, τ, is a function of the temperature and pressure of the heat bath and of the characteristics of the vibrating species. For practical purposes it was assumed that equation (21) was valid for any number of excited molecules and could be applied to a time varying heat bath as long as E_v^* and τ were taken as functions of the instantaneous state of the heat bath. Under these assumptions, τ should be technically referenced as a local relaxation time where numerical integration could produce a solution for a particular time span.

For sufficiently low temperatures the original Landau and Teller Theory [20] may be approximated by:

$$\tau = \frac{C}{P}\exp\left(\frac{K_2}{T}\right)^{1/3} \qquad (22)$$

where K is a constant dependent upon the physical properties of the species, and C is an empirical constant dependent upon the type of heat bath molecules.

In the present theoretical state, the evaluation of τ must be accomplished by experimental measurements interpreted in the light of the foregoing theoretical results. The methods of ultrasonic absorption, shock tube interferometry, spectroscopic data, and pressure measurement, have been used experimentally to produce the values of the constants for use in equation (22). These values are presented in Table II.

Taylor and Bitterman [18] present numerous graphs of both τ and the probability per collision of an exchange of energy between the translational and vibrational modes of a molecule.

Anderson, et al. [2], presents correlations between relaxation times, temperature and pressure for nitrogen and various collision partners. These correlations were utilized extensively and are therefore presented here.

$$\log_{10}(\tau P)_{N_2-N_2} = 93\ (T^{-1/3}) - 4.61 \qquad (23)$$

$$\log_{10}(\tau P)_{N_2-CO_2} = \log_{10}(\tau P)_{N_2-N_2} \qquad (24)$$

$$\log_{10}(\tau P)_{N_2-H_2O} = 15.4\ (T^{-1/3}) + 0.722 \qquad (25)$$

Bray [4] suggests that once an appreciable deviation from equilibrium has occurred that return to equilibrium in a nozzle is unlikely. Therefore, the investigation was centered on the stator nozzle block of the turbine. A stator passage with area change from throat to exit given by equation (26) and shown in Figure 3 was chosen,

$$A/A^* = 0.15x - 0.01x^2 \tag{26}$$

where A* was the area at the throat and x was the distance along the mid-span streamline measured from the throat. While the choice of this particular formula for change of passage area was arbitrary and not particularly critical, this choice is representative of modern turbines.

Knowledge of the area change and selection of a representative γ enabled determination of Mach number, and thermodynamic data from gas tables as presented in Table III. Selection of a total pressure and temperature at the burner outlet permitted evaluation of vibrational relaxation times at the throat of the stator with area change given by equation (26) for nitrogen to nitrogen collisions using equations (22), (23), or the graphs of Taylor and Bitterman [18]. (See Table IV.)

As stated previously, the calculated relaxation times had to be compared to a gas transit time. The gas transit (dwell) times were determined by dividing a characteristic length by the appropriate velocity. Under this concept, a total transit time was obtained by dividing the distance from point A to point B along the mid-span streamline by the mean velocity

between those two points. A local dwell time at a data point was obtained by dividing the distance between data points by the velocity at the upstream point.

Numerical evaluation of equation (21) was performed utilizing calculated relaxation times and the method of Hurle, Russo, and Hall [9]. The method is illustrated in Appendix C. This evaluation illustrated the actual amount of vibrational energy as compared to the equilibrium amount.

An aircraft gas turbine using hydrocarbon fuels will have many molecular species in the combustion products. It is known that some of these species are more effective for vibrational de-excitation. Consequently, a composite relaxation time involving several molecules was calculated. The molecular species in the combustion products were screened to ascertain the molecules most effective for vibrational de-excitation. This screening indicated H_2O and CO_2 should be included. A relaxation time was thus calculated for nitrogen with three different collision partners, N_2, CO_2, H_2O, using equations (23), (24), and (25) respectively (Table V). The total rate of change of vibrational energy of the nitrogen was considered to be the sum of three distinct quantities corresponding to the change induced by each of the collision partners.

$$\frac{dE_v}{dt}_{total} = A \frac{dE_v}{dt}_{N_2-N_2} + B \frac{dE_v}{dt}_{N_2-CO_2} + C \frac{dE_v}{dt}_{N_2-H_2O} \qquad (27)$$

Each of the terms on the right-hand side of this equation was expressed in the form of equation (21) and substituted to form equation (28)

$$\frac{dE_v}{dt_{total}} = A \frac{E_v^*-E_v}{\tau_{N_2-N_2}} + B \frac{E_v^*-E_v}{\tau_{N_2-CO_2}} + C \frac{E_v^*-E_v}{\tau_{N_2-H_2O}} \qquad (28)$$

The coefficients (A, B, C) were taken to be the mole fractions of the collision partner. Since the relaxation times with N_2 and CO_2 are equal, equation (28) may be expressed as

$$\frac{dE_v}{dt} = (E_v^*-E_v) \left[\frac{1 - X_{H_2O}}{\tau_{N_2-N_2}} + \frac{X_{H_2O}}{\tau_{N_2-H_2O}} \right] \qquad (29)$$

where X_{H_2O} is the mole fraction of water in a gas mixture. Comparing equation (29) with equation (21)

$$\frac{1}{\tau_{composite}} = \frac{1 - X_{H_2O}}{\tau_{N_2-N_2}} + \frac{X_{H_2O}}{\tau_{N_2-H_2O}} \qquad (30a)$$

The extension of equation (30a) to systems with a larger number of components is obvious. Note that E_v is the vibrational energy of nitrogen only. Values of τ composite are in Table VI.

Consider a large number of N_2^*, where N_2^* denotes vibrationally excited N_2. If the number of N_2^* exceeds the equilibrium value, there will be a decrease in the number of N_2^* as time progresses. The N_2^* may be de-excited by collisions with H_2O or CO_2 or N_2. The collision frequency with H_2O, CO_2, or N_2 depends upon the mole fraction. The probability that a given collision will result in de-excitation depends on the partners; i.e. on C and K_2 in equation (22). Using this physical picture, equations (27), (28), and (29) follow. In equation (29), each τ is evaluated at a pressure equal to that

exerted by the gas mixture. Alternately, an expression for τ composite would be

$$\frac{1}{\tau_{composite}} = \frac{1}{\tau_{N_2-N_2}} + \frac{1}{\tau_{N_2-H_2O}} \qquad (30b)$$

where partial pressures are used to evaluate τ for each species. The analogy of the equation for τ composite to the formula for resistances in parallel is apparent.

B. CHEMICAL NONEQUILIBRIUM FLOW

In order to investigate the effects and mechanics of chemical nonequilibrium on the flow in a turbine, the products of combustion of a stoichiometric reaction between air and a kerosine-type hydrocarbon fuel were considered and a turbine expansion calculation performed. The choice of a stoichiometric mixture ratio was indicated by the current trends and research goals in the turbojet industry. The internal degrees of freedom of all components of the gas were assumed to be in equilibrium throughout the expansion. Even though there is a known relationship between vibrational modes and chemical reaction, this assumption was necessary for analytical purposes.

The gas was taken as an inviscid, diffusionless fluid with quasi one-dimensional expansion through an ideal turbine. The process was considered to be adiabatic. The gas was expanded first as chemically frozen and then in full chemical equilibrium. The stations in the process were as illustrated in Figure 8. The concepts used in this section closely follow Penner's [13] development for chemically frozen flow.

In chemically frozen flow, the average molecular weight obviously remains constant; therefore, the work derived from this expansion can be expressed as

$$\text{Work}_{\text{frozen}} = \sum_{i=1}^{n} X_i (H_i(T_{t_1}) - H_i(T_{t_2})) \tag{31}$$

where X_i is the molar fraction of species i at station 1, n is the number of species present, and $H_i(T)$ is the total molar enthalpy of species i at temperature T.

Given values of P_{t_1}, T_{t_1}, and T_{t_2}, the total pressure at station two was determined from the isentropic relationship

$$P_{t_2} = P_{t_1} \left[\frac{T_{t_2}}{T_{t_1}} \right]^{\frac{\gamma^*}{\gamma^*-1}} \tag{32}$$

where γ^* is an appropriately defined average specific heat ratio during expansion. Penner [13] gives this ratio as:

$$\gamma^* = \frac{\sum_{i=1}^{n} X_i (S^\circ(T_{t_1}) - S^\circ(T_{t_2}))}{\sum_{i=1}^{n} X_i (S^\circ(T_{t_1}) - S^\circ(T_{t_2})) - \bar{R} \ln \frac{T_{t_1}}{T_{t_2}}} \tag{33}$$

The chemical nonequilibrium efficiency, η_c, was defined as the ratio of the work extracted from chemically frozen gas to the work extracted from equilibrium gas expanded to the same total pressure. This efficiency is

$$\eta_c = \frac{H_1 - H_2}{H_1 - H_3 \frac{\bar{M}_1}{\bar{M}_3}} \tag{34}$$

where

$$H_1 = \sum_{i=1}^{n} X_i(T_{t_1}, P_{t_1})H_i(T_{t_1}) \tag{35}$$

$$H_2 = \sum_{i=1}^{n} X_i(T_{t_1}, P_{t_1})H_i(T_{t_2}) \tag{36}$$

$$H_3 = \sum_{i=1}^{n} X_i(T_{t_3}, P_{t_3})H_i(T_{t_3}) \tag{37}$$

$$\overline{M}_1 = \sum_{i=1}^{n} X_i(T_{t_1}, P_{t_1})m_i \tag{38}$$

$$\overline{M}_3 = \sum_{i=1}^{n} X_i(T_{t_3}, P_{t_3})m_i \tag{39}$$

Once the quantities in the numerator of equation (34) were established as functions of known or given quantities, attention was focused on the denominator.

For equilibrium flow, the analysis was restricted to a given weight of gas mixture due to the temperature dependence of the average molecular weight of the mixture. For purposes of comparison it was convenient to choose the initial molecular weight of the gas mixtures as the characteristic weight; thus the ideal or equilibrium flow work was:

$$\text{Work}_{\text{equi}} = H_1 - \frac{\overline{M}_1}{\overline{M}_3} H_3 \tag{40}$$

where

$$H_1 = \sum_{i=1}^{n} X_i(T_{t_1}, Pt_1)\left[\Delta H^\circ_{f_i} + H_i(T_{t_1}) - H_i(T_o)\right] \tag{41}$$

and

$$H_3 = \sum_{i=1}^{n} X_i(T_{t_3}, P_{t_3}) \left[\Delta H^\circ_{f_i} + H_i(T_{t_1}) - H_i(T_o)\right] \qquad (42)$$

At this point, all the necessary quantities for evaluation of η_c were known except T_{t_3} which could be determined from isentropic considerations.

Isentropic flow occurred for the total weight of the gas mixture. Since $\bar{M}_1$ was chosen as the fixed weight for analysis, the isentropic relationship was:

$$\bar{S}(T_{t_1}, P_{t_1}) = \frac{\bar{M}_1}{\bar{M}_3} \bar{S}(T_{t_3}, P_{t_3}) \qquad (43)$$

$\bar{S}$ (T,P) is the molar entropy of an ideal gas mixture at temperature T and pressure P and may be expressed as

$$\bar{S}(T,P) = \sum_{i=1}^{n} X_i(T,P) S_i^\circ(T) - \bar{R}\left(\ell n\, P + \sum_{i=1}^{n} X_i(T,P)\, \ell n X_i(T,P)\right) \qquad (44)$$

where S°(T) is the molar entropy at temperature T and one atmosphere of pressure. Equations (44) and (44) were combined to yield

$$\sum_{i=1}^{n} X_i(T_{t_1}, P_{t_1}) \left[S_i^\circ(T_{t_1}) - \bar{R}\, \ell n\, P_{t_1} - \bar{R}\, \ell n\, X_i(T_{t_1}, P_{t_1})\right]$$
$$= \frac{\bar{M}_1}{\bar{M}_3} \sum_{i=1}^{n} X_i(T_{t_3}, P_{t_3}) \left[S_i^\circ(T_{t_3}) - \bar{R}\, \ell n\, P_{t_3} - \bar{R}\, \ell n\, X_i(T_{t_3}, P_{t_3})\right] \qquad (45)$$

This equation was used to solve for T_{t_3} by iteration. Once this has been accomplished, evaluation of equation (34) was possible.

The mechanics of the chemically reacting flow were then investigated. In the combustion chamber of a turbojet, a significant portion of the chemical energy released is used to break chemical bonds producing more elementary species. This energy is unavailable to do work unless it is first released through a recombination of the dissociated combustion products. The rate of each chemical reaction must be compared to a dwell time of the flow at any particular stage in order to determine the extent of the unavailability of energy.

Consider the typical three body reaction

$$A + B + M \underset{r_b}{\overset{r_f}{\rightleftarrows}} AB + M \qquad (46)$$

where M is a third body which removes energy during the recombination and r_f and r_b are reaction rates in the forward (recombination) and backward (dissociation) directions respectively. This equation represents two separate reactions with the connection that r_f must equal r_b at equilibrium. As the temperature and pressure move toward lower values during the expansion process, the reaction in equation (46) should move in the forward direction. If the reaction rate is not fast enough to maintain equilibrium conditions, recombination will lag, and the gas driving the turbine will have dissociated products whose dissociation energy has not contributed to the kinetic energy of the flow. The lag of recombination results in a reduction of performance.

Equilibrium flow calculations involve the simultaneous solution of the conservation equations for mass, energy,

momentum, and species, plus the equation of state. This system is simplified for frozen flow because the species composition is constant. Computer programs for solution of equilibrium and nonequilibrium flows are presented by Gordon and Zeleznik [8] and Zupnik, et al., [23].

For relaxing flow in a turbine the problem is complex because the nonlinear kinetic differential equations of species concentration and the conservation of atom equations are now involved. Solution of the chemical relaxation problem is obviously desirable but beyond the scope of the present investigation. Penner [12] and Bray [4] have proposed criteria to determine when the shift may be made from equilibrium to nonequilibrium analysis. Application of these criteria by various researchers has produced varied degrees of success.

Newhall [10] presents twenty-eight elementary reactions (Table X) that may be considered significant in the flow of combustion products resulting from a mixture of a hydrocarbon fuel and air. These equations may be integrated numerically with the coupled energy equation to produce concentration-time histories for each species during expansion, but this was beyond the scope of this thesis.

The science of chemical kinetics, the study of the rates of chemical reactions, is complex and difficult, both experimentally and theoretically. A discussion of both simple collisional theory and transition state theory is given in Pratt [14] and emphasizes the heavy reliance, except in the simplest reactions, upon empirical data.

The chemical reaction rate may be considered to be proportional to the total number of collisions between reacting chemical species and to the fraction of this total in which sufficient energy is available for the reaction to occur. In flow systems the rate of reaction is also dependent on the mass and energy transport mechanisms. The collision rate is dependent upon both concentration and effective collision cross section of the molecules involved.

The most widely utilized approach to the reaction rate problem is through the use of the Arrhenius equation

$$K = A(T)\ \exp(-E_a/RT) \tag{47}$$

where A is the pre-exponential factor and E_a is the experimental activation energy. The values of both A and E_a are obtained from experimental plots of ℓn K vs 1/T. Both A and E_a may be functions of temperature.

For elementary reactions, such as those that make up the complex reactions in the combustion products, the rate constant, K, from the Arrhenius equation (47) may be employed as follows: The rate of change in the concentration of a product AB produced by a reaction such as equation (46).

$$A + B + M \rightleftarrows AB + M \tag{46}$$

is equal to

$$\frac{d\ (AB)}{dt} = K\ (A)\ (B)\ (M) \tag{48}$$

for an elementary reaction where the parentheses signify concentration in moles per cc.

Each of the equations in Table X had corresponding forward and backward rate constants from Table XI. Each of these rate constants was calculated at the throat of the turbine stator model introduced previously (Table XII). The mole fractions of the species in the combustion products were calculated at the stator throat using Banes, et al., [3] and are presented in Tables XIII and XIV. A conversion factor that enabled the use of mole fractions instead of molar concentrations in equation (48) was developed and is presented in Appendix D. The reaction rates for the equations considered were calculated at the stator throat and are tabulated in Table XV. The total reaction rate for each specie was determined by a summation of the rate of destruction or creation of the specie from the applicable equation. If the particular specie appeared on the left-hand side of the reaction equation in Table X it was considered as being destroyed at the forward rate and produced at the backward. In Table XI, the total reaction rate at the stator throat for each specie is presented.

The determination of the presence of chemically frozen flow in the turbine required establishment of a characteristic reaction time. The total reaction rate, R_i, of a specie i, had units of moles $\sec^{-1}$ cm^{-3}. Multiplying R_i by the specie molecular weight produced units of grams of i per cm^3 per sec, which yields a rate of change of density.

$$R_i \ m_i \ = \ \frac{d\rho_i}{dt} \tag{49}$$

By taking the gas average density at the throat, $\overline{\rho}_i$, and

dividing both sides of equation (49) by $\overline{\rho}_i$, a rate of change of mass fraction is obtained for small mixture density changes.

$$\frac{R_i \; m_i}{\overline{\rho}_i} = \frac{1}{\overline{\rho}_i} \frac{d\rho_i}{dt} \simeq \frac{dY_i}{dt} \qquad (50)$$

By definition

$$Y_i = \frac{m_i}{\overline{M}} X_i \qquad (51)$$

For sufficiently small changes

$$\frac{dY_i}{dt} \cong \frac{Y_{i_2} - Y_{i_1}}{t_2 - t_1} \qquad (52)$$

Letting $t_2 - t_1 \equiv t_{r_i}$ equation (50) may be rewritten as

$$\frac{R_i \; m_i}{\overline{\rho}_1} = \frac{dY_i}{dt} = \frac{Y_{i_2} - Y_{i_1}}{t_{R_i}}$$

or

$$t_{R_i} = \frac{X_{i_2} \dfrac{m_i}{\overline{M}_2} - X_{i_1} \dfrac{m_i}{\overline{M}_1}}{\dfrac{R_i \; m_i}{\overline{\rho}_1}} \qquad (53)$$

Rearranging

$$t_{R_i} = \frac{\overline{\rho}_1}{R_i} \left[\frac{X_{i_2}}{\overline{M}_2} - \frac{X_{i_1}}{\overline{M}_1} \right] \qquad (54)$$

Evaluation of equation (54) provided a basis for comparing reaction times with dwell times.

III. RESULTS AND DISCUSSION

Values of the vibrational efficiency defined by equation (16) were calculated using stagnation conditions of 2200°K and 20 Atmospheres. These values are presented in Table I. The data in Table I are plotted in Figure 4 as loss percentage against the change of total temperature of the RT gas from stations 1 and 2. See Figure 1 for station numbering. Selection of this abscissa illustrates the variance of the vibrational efficiency with the amount of work extracted.

The data for different Mach numbers indicates that this efficiency as defined is a definite function of turbine exit Mach number. It is known that for a given static temperature there is a known amount of energy stored in the vibrational mode of internal energy at equilibrium. As the exit Mach number increases, the kinetic energy extracts a larger portion of the rotational and translational energy depicted in Figure 2. Therefore, the static temperature of the RT gas is lower and the amount of equilibrium vibrational energy is lower. The total vibrational energy at the turbine exit is the same as the equilibrium vibrational energy at the burner outlet. As the Mach number increases, the RT gas static temperature decreases and the fraction of the total vibrational energy at the exit that corresponds to the RT gas temperature decreases. Therefore, the flow experiences a larger departure from equilibrium and an attendant increase in the losses.

The apparent minima of curves in Figure 4 as indicated by the dashed line is a result of the mechanism of work removal. The work was extracted from a RT gas which had both modes fully excited in the temperature range considered. This full excitation made the work extraction a linear function of temperature. The equilibrium work in the denominator of equation (15) was drawn from all modes of the gas. At the temperatures considered, vibrational specific heat is nonlinear and is the apparent cause of the minima.

There were three sources of vibrational relaxation times: equation (22), the graphs of Taylor and Bitterman [18], and the equations of Anderson, et al., [2]. In Table IV, relaxation times for nitrogen-nitrogen collisions are calculated by the three methods. The values are for an area change as defined in equation (26) and stagnation conditions of 2200°K and 20 atmospheres. The variation in the values of relaxation time when calculated by the three methods indicates that the data basis for each calculating method is different. The graphs of Taylor and Bitterman [18] had insufficient range for this analysis. The values obtained through the use of equation (22) seem unusually small and therefore were not used. The Anderson, et al., [2] data is a later development with information for many different collision partners, and its use allowed more flexibility of investigation.

The relaxation times for nitrogen as a function of stator area ratio are given in Table V for a stagnation temperature of 2200°K and various stagnation pressure ranging from 5 to 20 atmospheres. Equation (26) was used to calculate area ratio

as a function of distance along the midspan streamline. These data are plotted in Figure 5 with the area ratio as the abscissa. The area ratio values are of significance only in that they define data collection points. The pressure dependence of the relaxation is aptly demonstrated in this figure. The lower pressure results in a lower collision frequency and thereby slows the relaxation. The curve of relaxation time for nitrogen-water collisions emphasizes the catalytic effect of water on the relaxation process. The presence of water in the combustion products of a hydrocarbon and air mixture helps to delay the onset of vibrational freezing.

The dwell time as plotted in Figure 5 represents the reciprocal of the local velocity in units of seconds per inch multiplied by a factor of ten. The order of magnitude of the dwell time was raised because exact numerical solution of equation (21) indicated vibrational freezing is significant at $A/A^* = 1.14$. The factor of ten multiplication results in the dwell time and relaxation time curve intersection agreeing with that solution. The multiplication factor makes the dwell time longer and more pessimistic. The intersection of the dwell time curve with the relaxation time curves represents a position downstream of which the flow may be considered to be vibrationally frozen. For the pure nitrogen, this point occurs at a low area ratio indicating that the flow is probably fully frozen for practical calculations. Once the flow has frozen, Bray [4] indicates that it will remain frozen or at least in some form of nonequilibrium. The fact that

freezing is indicated early in the stator section of the turbine implies that the flow should be considered as vibrationally frozen throughout the turbine performance calculations.

Equation (21) was evaluated for various conditions and the data plotted in Figures 6 and 7. Both of these figures dramatically demonstrate the departure from vibrational equilibrium that occurs at a low area ratio. The effects of other collision partners are shown in Figure 7 using data from Tables VII and VIII. The upward movement of the curve in Figure 7 when the midspan streamline length is reduced is a result of a lower gas transit time.

Values of the chemical nonequilibrium efficiency were computed from equation (34) for stagnation conditions of 2200°K and 20 atmospheres of pressure at the burner outlet. These values are presented in Table IX. Data from Table IX were plotted as loss percentage in Figure 9 with the change of total temperature from burner outlet to turbine exit as the abscissa. Here again the total temperature change is an indicator of the amount of work extracted. The losses due to chemical freezing in this stoichiometric-mixture expansion are rather low. For the temperature range considered, the amount of nitrogen dissociation is negligible. This is significant because nitrogen comprises nearly three-quarters of the gas mixture. For the stoichiometric mixture there is very little oxygen remaining to dissociate after the reaction. Considering the size of the losses, the tendencies of the curve are

subject to question. The precision of the thermochemical data utilized for the calculation would have significant effect on the results.

The characteristic reaction time for each specie was calculated from equation (54) using the data for the stator throat and stator exit at total temperature of 2200°K and total pressures of 15 and 5 atmospheres. These times are in Table XVIII. Only the reactions considered to be the fastest were utilized in the analysis. The influence of slower reactions upon the fast reactions was not analyzed. Each of the times was analyzed and a classification was performed. The gas transit time from stator throat to exit was compared to each specie reaction time, and the specie was placed in an appropriate section of Table XIX.

A negative reaction time for a specie indicated that the predominate or fast reactions involving that specie were away from equilibrium for the particular conditions of temperature, pressure and concentrations. The real life case, including reactions not considered here, would, for long time periods, cause the reaction times to become positive. The negative reaction time species were classified as frozen. A long or short positive reaction time compared to the transit time classified the specie as frozen or equilibrium respectively. Specie reaction times of the same order of magnitude as the transit times were classified as unknown. The approximation used to calculate the reaction times was not sufficiently accurate to make a definite statement as to the freezing of

the particular specie. Table XIX definitely indicates the presence of chemically near-frozen flow.

Several aspects of the current state of the art in turbojet development tend to reinforce the gravity of the losses calculated in this paper. As the aircraft operate at higher and higher altitudes, the total pressure at the burner outlet will decrease. This will insure the presence of vibrational and chemical nonequilibrium as illustrated in Figure 5, 6, 7, and Table XIX. The use of hydrogen fuel would produce large amounts of water thereby delaying the vibrational freezing effects. The magnitude of the burner outlet temperature will vary as the ability of the turbine blade cooling method to handle high inlet temperature, and this variation will effect the degree of nonequilibrium present.

IV. CONCLUSIONS

The vibrational freezing of the flow in the turbine section of an advanced turbojet using a stoichiometric mixture of kerosine and air can result in losses of up to seven percent when compared to equilibrium flow.

The vibrational freezing of the flow will be virtually complete a short distance after the throat of the first stator assembly.

The losses due to chemical freezing are insignificant compared to the vibrational freezing losses.

APPENDIX A

TABLE I

VIBRATIONAL EFFICIENCY WITH TOTAL TEMPERATURE OF 2200°K AND TOTAL PRESSURE OF 20 ATM

T'_2, °K	$M'_2 = .1$	$M'_2 = .3$	$M'_2 = .5$
1500	96.37	95.21	92.66
1550	96.85	95.40	92.63
1600	97.00	95.52	92.49
1650	97.27	95.95	92.43
1700	97.71	95.89	92.02
1750	97.90	95.80	91.62
1800	97.98	95.80	91.03
1850	97.81	95.43	90.51
1900	98.14	95.14	89.46

TABLE II

VALUES OF CONSTANTS FOR USE IN EQUATION (22) FROM VINCENTI AND KRUGER [20]

Species	Heat Bath Molecules	C Atm-microsec	K_2 °K	Approximate Range of T °K
O_2	O_2	5.42×10^{-5}	2.95×10^{6}	800 - 3200
O_2	Ar	3.5×10^{-4}	2.95×10^{6}	1300 - 4300
N_2	N_2	7.12×10^{-3}	1.91×10^{6}	800 - 6000
NO	NO	4.86×10^{-3}	1.37×10^{5}	1500 - 3000
NO	NO	6.16×10^{-1}	1.37×10^{5}	1500 - 4600

TABLE III

STATOR AREA CHANGE WITH ASSOCIATED IDEAL GAS DATA FROM WANG, ET AL. [21]

$\gamma = 1.26$

A/A*	M	T/T_t	P/P_t	Velocity, M/sec	Dwell Time, sec/in
1	1.0	.885	.5531	854	29.7
1.14	1.43	.791	.3191	1154	22
1.27	1.59	.7526	.2523	1252	20.3
1.37	1.69	.7292	.217	1310	19.4
1.46	1.77	.7106	.1925	1354	18.8
1.51	1.81	.702	.18	1376	18.5
1.55	1.83	.696	.172	1389	18.3

TABLE IV

COMPARISON BETWEEN VARIOUS METHODS OF OBTAINING STATOR RELAXATION TIMES WITH TOTAL TEMPERATURE = 2200°K AND TOTAL PRESSURE = 15 ATM

A/A*	T	P	τ Eqn. (22)	τ Graphs	τ Eqn. (23)
1	1947	11.06	13.3	63.3	61.1
1.14	1740	6.38	33.7	172.4	207.5
1.27	1656	5.05	50.6	238	353
1.37	1604	4.34	65.8	**	498
1.48	1563	3.85	81.3	**	658
1.51	1544	3.60	90.8	**	759
1.55	1531	3.44	98	**	837

** Unable to extrapolate the graph further.

TABLE V

STATOR RELAXATION TIMES IN MICRO-SECONDS OF NITROGEN MOLECULES UNDER VARIED TOTAL PRESSURES WITH TOTAL TEMPERATURE = 2200°K USING EQUATION (23)

A/A*	Pressure, Atm				
	20	15	15	10	5
			**		
1	61.1	82.9	10.8	124	249
1.14	207.5	277	21	415	830
1.27	353	471	28	706	1412
1.37	498	663	33	996	1992
1.46	658	876	39	1316	2631
1.51	759	1011	42	1577	3035
1.55	837	1116	44	1673	3347

** Collision Partner is H_2O in this column vice N_2 as in the other columns.

TABLE VI

COMPOSITE RELAXATION TIMES CALCULATED USING EQUATION (30a) WITH TOTAL PRESSURE = 15 ATM

A/A*	N_2-N_2	H_2O-N_2	Composite
1	82.9	10.8	44.2
1.14	277	21	106.4
1.27	471	27.9	152.5
1.37	663	33.4	190.6
1.46	876	38.7	228
1.51	1011	42	250.5
1.55	1116	44.3	267

TABLE VII

RATIO OF ACTUAL VIBRATIONAL ENERGY TO EQUILIBRIUM VIBRATIONAL ENERGY AT THE THROAT UNDER VARIOUS TOTAL PRESSURES AT TOTAL TEMPERATURE = 2200°K

Total Pressure, ATM	$\frac{E^*_v}{E^*_{v_{th}}}$	A/A*	$\frac{E_v}{E^*_{v_{th}}}$	Total Pressure	A/A*	$\frac{E_v}{E^*_{v_{th}}}$
20	1	1	1	10	1	1
	.8388	1.14	.9919		1.14	.9958
	.7733	1.27	.9779		1.27	.9886
	.7331	1.37	.9634		1.37	.9831
	.7006	1.46	.9553		1.46	.9786
	.6856	1.51	.9485		1.51	.9749
	.6755	1.55	.9423		1.55	.9715
15		1	1	5	1	1
		1.14	.9938		1.14	.9979
		1.27	.9832		1.27	.9942
		1.37	.9751		1.37	.9914
		1.46	.9687		1.46	.9891
		1.51	.9633		1.51	.9871
		1.55	.9584		1.55	.9854

TABLE VIII

RATIO OF ACTUAL VIBRATIONAL ENERGY TO EQUILIBRIUM VITRATIONAL ENERGY AT THE THROAT WITH TOTAL PRESSURE = 15 ATM AND TOTAL TEMPERATURE = 2200°K FOR VARIOUS MIDSPAN STREAMLINE LENGTHS

$\frac{E_v^*}{E_{v_{th}}^*}$	A/A*	$\frac{E_v}{E_{v_{th}}^*}$ †	$\frac{E_v}{E_{v_{th}}^*}$ ††	$\frac{E_v}{E_{v_{th}}^*}$ †††
1	1	1	1	1
.8388	1.14	.9938	.9979	.9946
.7733	1.27	.9832	.9942	.9846
.7731	1.37	.9751	.9914	.9758
.7706	1.46	.9687	.9891	.9680
.6856	1.51	.9633	.9871	.9609
.6755	1.55	.9584	.9854	.9544

† : Midspan streamline length is 6"; collision Partner N_2.

†† : Midspan streamline length is 2"; collision Partner N_2.

††† : Midspan streamline length is 2"; collision Partners, N_2, CO_2 and H_2O.

TABLE IX

CHEMICAL EFFICIENCY CALCULATED USING EQUATION (34) WITH TOTAL TEMPERATURE = 2200°K

Turbine Exit Total Temperature	η_c
1500	98.92
1600	99.00
1700	99.15
1800	99.15
1900	99.50

TABLE X

ELEMENTARY CHEMICAL REACTIONS FROM NEWHALL [10]

1.	H_2O	+	M	$\rightleftarrows$	OH	+	H	+	M
2.	H_2	+	M	$\rightleftarrows$	H	+	H	+	M
3.	NO	+	M	$\rightleftarrows$	N	+	O	+	M
4.	N_2	+	M	$\rightleftarrows$	N	+	N	+	M
5.	NO_2	+	M	$\rightleftarrows$	NO	+	O	+	M
6.	O_2	+	M	$\rightleftarrows$	O	+	O	+	M
7.	OH	+	H	$\rightleftarrows$	H_2	+	O		
8.	OH	+	O	$\rightleftarrows$	O_2	+	H		
9.	OH	+	H_2	$\rightleftarrows$	H_2O	+	H		
10.	OH	+	OH	$\rightleftarrows$	H_2O	+	O		
11.	CO	+	OH	$\rightleftarrows$	CO_2	+	H		
12.	NO	+	O	$\rightleftarrows$	O_2	+	N		
13.	NO	+	N	$\rightleftarrows$	N_2	+	O		
14.	NO	+	O_2	$\rightleftarrows$	NO_2	+	O		

TABLE XI

SELECTED RATE CONSTANTS FOR THE ELEMENTARY CHEMICAL REACTIONS FROM NEWHALL [10]

Reaction	Forward Rate Constant	Backward Rate Constant
1	$5.4 \times 10^{17} \exp(-123{,}600/RT)$	1.5×10^{16}
2	$3.1 \times 10^{15} \exp(-110{,}000/RT)$	$7.0 \times 10^{17} / T$
3	$\frac{7 \times 10^{10}}{T^{1/2}} \frac{(150{,}000)^2}{(RT)^2} \exp(-150{,}000/RT)$	9.0×10^{14}
4	$\frac{4.2 \times 10^{12}}{T^{1/2}} \left(\frac{224{,}900}{RT}\right) \exp(-224{,}900/RT)$	6.1×10^{14}
5	$\frac{5.4 \times 10^{21}}{T} \exp(-74{,}000/RT)$	2.0×10^{16}
6	$6 \times 10^{13} \frac{118{,}000}{RT} \exp(-11{,}800/RT)$	1.0×10^{14}
7	$1.4 \times 10^{12} \exp(-6{,}000/RT)$	$3.3 \times 10^{12} \exp(-8{,}000/RT)$
8	$5.5 \times 10^{13} \exp(-1{,}000/RT)$	$7.2 \times 10^{14} \exp(-16{,}900/RT)$
9	$6.2 \times 10^{13} \exp(-6{,}000/RT)$	$3.2 \times 10^{14} \exp(-21{,}100/RT)$
10	$7.7 \times 10^{12} \exp(-1{,}000/RT)$	$8.3 \times 10^{13} \exp(-18{,}100/RT)$
11	$7.1 \times 10^{12} \exp(-7{,}700/RT)$	$4.7 \times 10^{14} \exp(-27{,}250/RT)$
12	$3.2 \times 10^{9} \exp(-39{,}100/RT)$	$13.3 \times 10^{9} \exp(-7{,}080/RT)$
13	1.55×10^{13}	$7 \times 10^{13} \exp(-75{,}500/RT)$
14	$1.8 \times 10^{10} T^{1/2} \exp(-47{,}000/RT)$	$5.8 \times 10^{10} \; T^{1/2}$

TABLE XII

RATE CONSTANTS AT 1947°K

Reaction	Forward Constant	Backward Constant
1	7.1979×10^{3}	1.5×10^{16}
2	1.3896×10^{3}	3.5933×10^{14}
3	3.4565×10^{-5}	9.0×10^{15}
4	6.1003×10^{-10}	6.1×10^{14}
5	1.36733×10^{10}	2.0×10^{16}
6	1.037×10^{2}	1.0×10^{14}
7	2.9688×10^{11}	4.17295×10^{11}
8	4.247×10^{13}	9.1234×10^{12}
9	1.3147×10^{13}	1.3693×10^{12}
10	5.9461×10^{12}	7.7125×10^{11}
11	9.702×10^{11}	4.1025×10^{11}
12	2.542×10^{8}	4.1536×10^{12}
13	1.55×10^{13}	2.3418×10^{5}
14	4.205×10^{6}	2.559×10^{12}

TABLE XIII

EQUILIBRIUM MOLE FRACTIONS WITH TOTAL TEMPERATURE = 2200°K AND TOTAL PRESSURE = 15 ATM FROM BANES, ET AL., [3]

	Throat	Exit
T	1947°K	1531°K
P	8.3 atm	2.58 atm
CO_2	1.2919×10^{-1}	1.3073×10^{-1}
H_2O	1.2992×10^{-1}	1.3048×10^{-1}
O_2	6.7092×10^{-4}	5.3073×10^{-5}
H_2	3.4679×10^{-4}	3.6215×10^{-5}
N_2	7.2896×10^{-1}	7.2981×10^{-1}
N	1×10^{-12}	1×10^{-12}
NO	3.8768×10^{-4}	2.4451×10^{-5}
OH	2.5755×10^{-4}	1.2768×10^{-5}
CO	1.4098×10^{-3}	1.0068×10^{-4}
NO_2	1.1142×10^{-7}	2.8080×10^{-9}
H	7.9334×10^{-6}	1.2395×10^{-7}
O	4.4208×10^{-6}	3.8529×10^{-6}
$\overline{M}$	28.876	28.903
$\overline{\rho}$	1.499×10^{-3}	5.938×10^{-4}

TABLE XIV

EQUILIBRIUM MOLE FRACTIONS WITH TOTAL TEMPERATURE = 2200°K AND TOTAL PRESSURE = 5 ATM FROM BANES, ET AL., [3]

	Throat	Exit
T	1947°K	1531°K
P	2.7655 atm	0.86 atm
CO_2	$1.2845\text{x}10^{-1}$	$1.3068\text{x}10^{-1}$
H_2O	$1.2963\text{x}10^{-1}$	$1.3045\text{x}10^{-1}$
O_2	$1.0156\text{x}10^{-3}$	$7.6494\text{x}10^{-5}$
H_2	$5.0574\text{x}10^{-4}$	$5.0628\text{x}10^{-5}$
N_2	$7.2857\text{x}10^{-1}$	$7.2979\text{x}10^{-1}$
N	$1\text{x}10^{-12}$	$1\text{x}10^{-12}$
NO	$4.7613\text{x}10^{-4}$	$2.9394\text{x}10^{-5}$
OH	$3.8269\text{x}10^{-4}$	$1.8211\text{x}10^{-5}$
CO	$2.1936\text{x}10^{-3}$	$1.7399\text{x}10^{-4}$
NO_2	$9.4140\text{x}10^{-8}$	$2.4052\text{x}10^{-9}$
H	$1.7402\text{x}10^{-5}$	$2.4370\text{x}10^{-7}$
O	$9.8841\text{x}10^{-6}$	$7.6885\text{x}10^{-8}$
$\overline{M}$	28.863	28.902
$\overline{\rho}$	$4.997\text{x}10^{-4}$	$1.98\text{x}10^{-4}$

TABLE XV

REACTIONS RATES OF ELEMENTARY EQUATIONS AT 1947°K

Total Pressure, Atm	15		5	
	Forward	Backward	Forward	Backward
1	$1.839\text{x}10^{-6}$	$3.132\text{x}10^{-6}$	$2.037\text{x}10^{-7}$	$3.775\text{x}10^{-7}$
2	$9.48\text{x}10^{-10}$	2.3127x10	$1.534\text{x}10^{-10}$	$4.114\text{x}10^{-10}$
3	$2.636\text{x}10^{-17}$	$4.066\text{x}10^{-16}$	$3.593\text{x}10^{-18}$	$3.36\text{x}10^{-16}$
4	$8.748\text{x}10^{-19}$	$1.02\text{x}10^{-37}$	$9.703\text{x}10^{-20}$	$2.305\text{x}10^{-24}$
5	$2.997\text{x}10^{-6}$	$3.503\text{x}10^{-6}$	$2.81\text{x}10^{-7}$	$3.56\text{x}10^{-7}$
6	$1.369\text{x}10^{-10}$	$1.997\text{x}10^{-10}$	$2.30\text{x}10^{-11}$	$3.69\text{x}10^{-11}$
7	$1.637\text{x}10^{-6}$	$1.727\text{x}10^{-6}$	$5.92\text{x}10^{-7}$	$6.25\text{x}10^{-7}$
8	$1.305\text{x}10^{-4}$	$1.31\text{x}10^{-4}$	$4.81\text{x}10^{-5}$	$4.83\text{x}10^{-5}$
9	$3.169\text{x}10^{-3}$	$3.809\text{x}10^{-3}$	$7.62\text{x}10^{-4}$	$9.26\text{x}10^{-4}$
10	$1.064\text{x}10^{-3}$	$1.1955\text{x}10^{-3}$	$2.61\text{x}10^{-4}$	$2.28\text{x}10^{-3}$
11	$1.018\text{x}10^{-3}$	$1.1348\text{x}10^{-3}$	$2.44\text{x}10^{-4}$	$2.75\text{x}10^{-4}$
12	$1.176\text{x}10^{-9}$	$7.52\text{x}10^{-12}$	$3.58\text{x}10^{-10}$	$1.26\text{x}10^{-12}$
13	$1.620\text{x}10^{-11}$	$2.04\text{x}10^{-9}$	$2.21\text{x}10^{-12}$	$5.05\text{x}10^{-10}$
14	$2.952\text{x}10^{-9}$	$3.40\text{x}10^{-9}$	$6.09\text{x}10^{-10}$	$7.14\text{x}10^{-10}$

TABLE XVI

EQUATIONS FOR TOTAL REACTION RATE OF EACH SPECIE

$$R_{CO_2} = r_{11f}-r_{11b}$$

$$R_{H_2O} = r_{1b}-r_{1f}+r_{9f}-r_{9b}+r_{10f}-r_{11b}$$

$$R_{O_2} = r_{6b}-r_{6f}+r_{8f}-r_{8b}+r_{12f}-r_{12b}+r_{14b}-r_{14f}$$

$$R_{H_2} = r_{2b}-r_{2f}+r_{7f}-r_{7b}+r_{9b}-r_{9f}$$

$$R_{N_2} = r_{4b}-r_{4f}+r_{13f}-r_{13b}$$

$$R_{NO} = r_{3b}-r_{3f}+r_{5f}-r_{5b}+r_{12b}-r_{12f}+r_{13b}-r_{13f}+r_{14b}-r_{14f}$$

$$R_{OH} = r_{1f}-r_{1b}+r_{7b}-r_{7f}+r_{8b}-r_{8f}+r_{9b}-r_{9f}+2r_{10b}-2r_{10f}+r_{11b}-r_{11f}$$

$$R_{CO} = r_{11b} - r_{11f}$$

$$R_{NO_2} = r_{5b}-r_{5f}+r_{14f}-r_{14b}$$

$$R_{H} = r_{1f}-r_{1b}+2r_{2f}-2r_{2b}+r_{7b}-r_{7f}+r_{8f}-r_{8b}+r_{9f}-r_{9b}+r_{11f}-r_{11b}$$

$$R_{O} = r_{3f}-r_{3b}+r_{5f}-R_{5b}+2r_{6f}-2r_{6b}+r_{7f}-r_{7b}+r_{8b}-r_{8f}+r_{10f}-r_{10b}$$
$$+r_{12b}-r_{12f}+r_{13f}-r_{13b}+r_{14f}-r_{14b}$$

TABLE XVII

TOTAL REACTION RATE, R, AT THE THROAT WITH STATIC TEMPERATURE = 1947°K

Species	Total Pressure	
	15	5
CO_2	$- 1.168\times10^{-4}$	$- 3.13\times10^{-5}$
H_2O	$- 7.7\times10^{-4}$	$- 2.185\times10^{-3}$
O_2	$- 4.98\times10^{-7}$	$- 1.695\times10^{-7}$
H_2	6.4×10^{-4}	1.63×10^{-4}
N_2	$- 2.02\times10^{-9}$	$- 5.03\times10^{-10}$
NO	$- 5.047\times10^{-7}$	$- 7.445\times10^{-8}$
OH	1.019×10^{-3}	4.24×10^{-3}
CO	1.168×10^{-4}	3.13×10^{-5}
NO_2	5.056×10^{-7}	7.46×10^{-8}
H	$- 7.59\times10^{-4}$	$- 1.95\times10^{-4}$
O	$- 1.316\times10^{-4}$	$- 2.022\times10^{-3}$

TABLE XVIII

CHARACTERISTIC REACTION TIMES IN THE THROAT AREA IN ORDER TO REACH EXIT EQUILIBRIUM CONDITIONS FOR TOTAL TEMPERATURE = 2200°K

	Total Pressure	
	15	5
Species	Time	
CO_2	$+ 6.3\times10^{-4}$	$+ 1.14$
H_2O	$+ 2.95\times10^{-5}$	$- 5.1\times10^{-3}$
O_2	$- 6.44\times10^{-2}$	$- 9.59\times10^{1}$
H_2	$+ 2.52\times10^{-5}$	$+ 4.84\times10^{-2}$
N_2	$+ 4.32$	$+ 8.10\times10^{3}$
NO	$- 3.74\times10^{-2}$	$- 1.04\times10^{2}$
OH	$+ 1.25\times10^{-5}$	$+ 1.49\times10^{-3}$
CO	$+ 6.26\times10^{-4}$	$+ 2.00\times10^{1}$
NO_2	$+ 1.12\times10^{-5}$	$+ 3.62\times10^{-1}$
H	$- 5.34\times10^{-7}$	$- 2.56\times10^{-2}$
O	$- 1.73\times10^{-6}$	$- 1.40\times10^{-3}$
Transit Time	5.7×10^{-5}	

TABLE XIX

FREEZING CLASSIFICATION OF CHEMICAL SPECIES

Total Pressure	Frozen	Unknown	Equilibrium
15	O_2 N_2 NO H O	H_2O CO_2 H_2 OH CO NO_2	None
5	H_2O CO_2 O_2 H_2 N_2 NO OH CO NO_2 H O	None	None

APPENDIX B

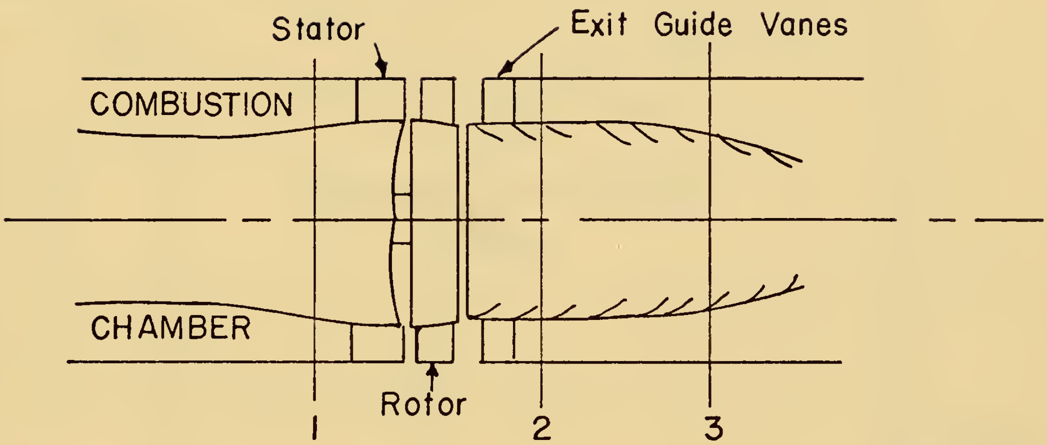

FIGURE I TURBINE SCHEMATIC AND FLOW STATION IDENTIFICATION FOR THE VIBRATIONAL FREEZING ANALYSIS

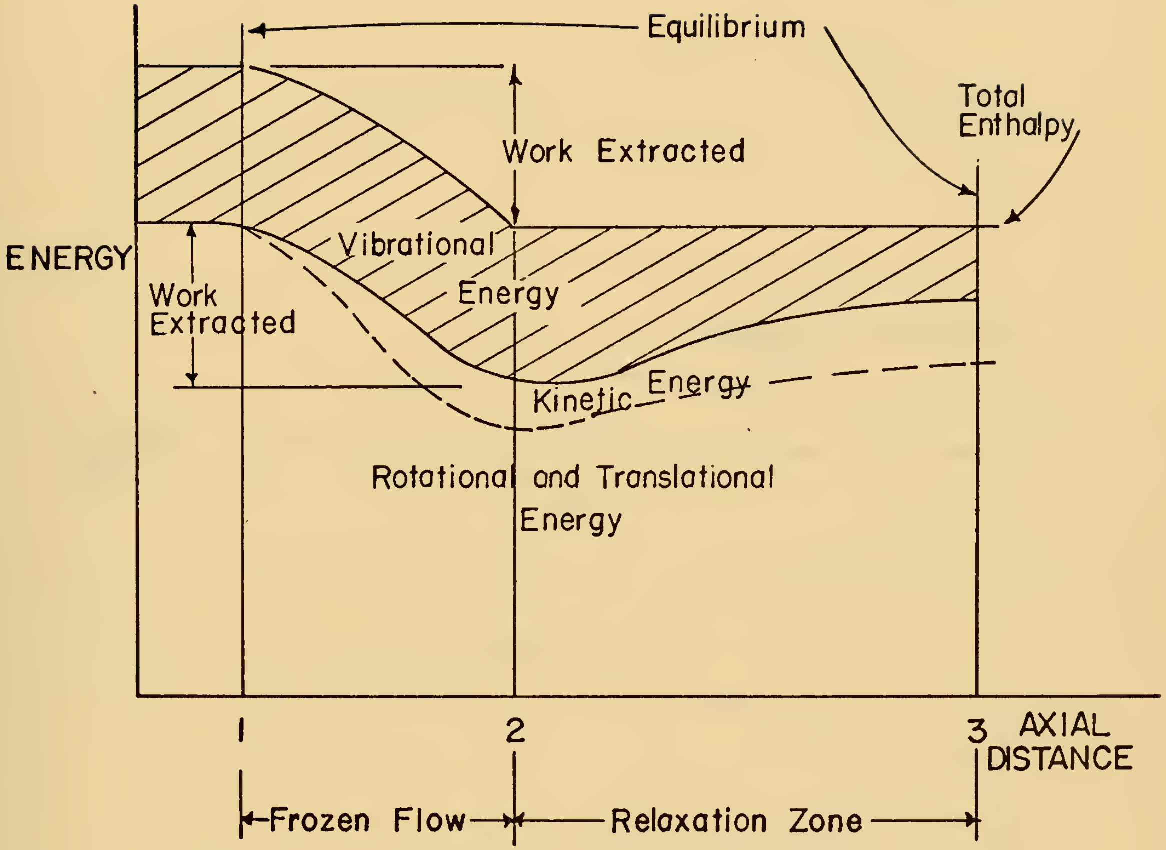

FIGURE 2 ENERGY DISTRIBUTION IN THE TURBINE FOR THE VIBRATIONAL FREEZING ANALYSIS

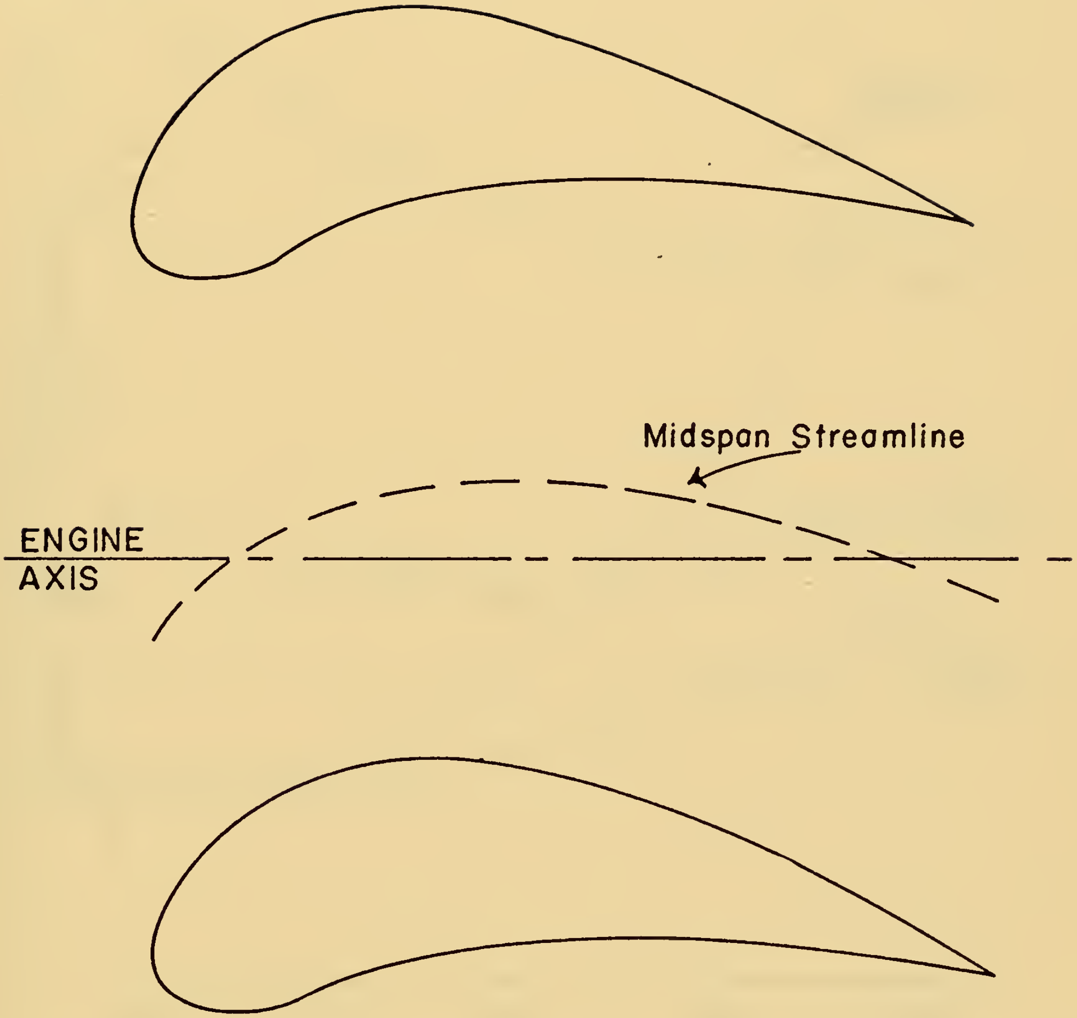

FIGURE 3   STATOR PASSAGE

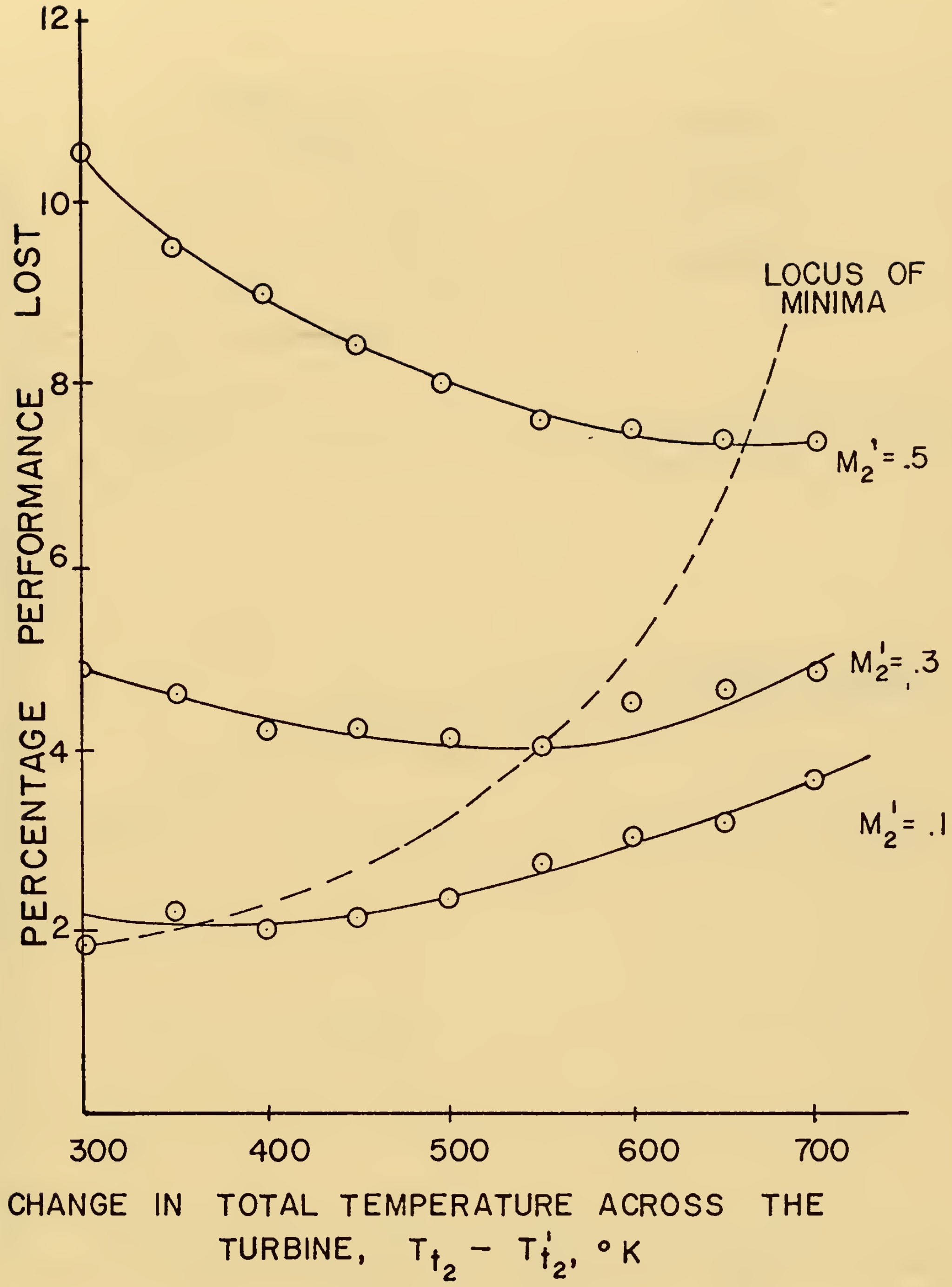

FIGURE 4 PERCENTAGE PERFORMANCE LOST DUE TO VIBRATIONAL FREEZING

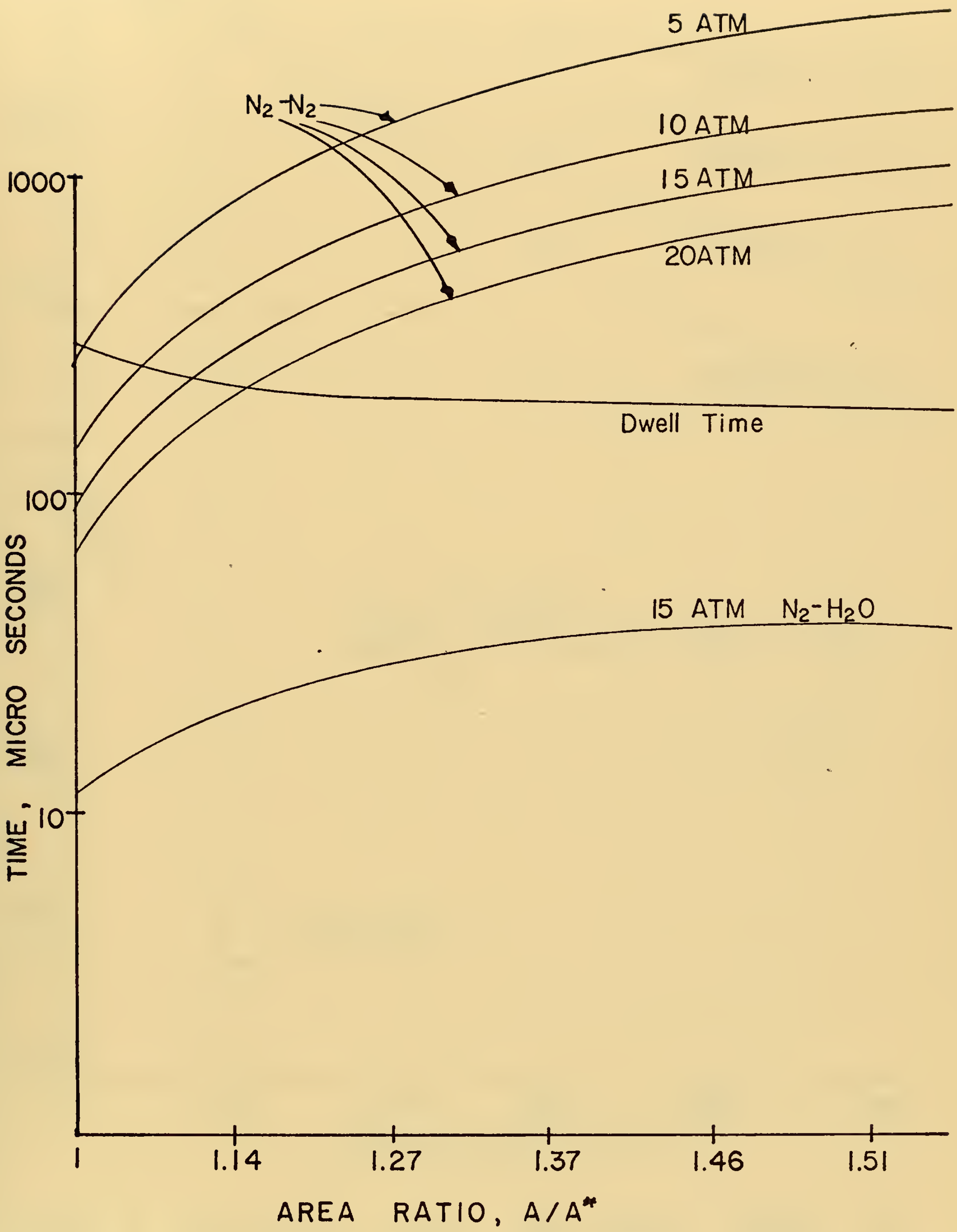

FIGURE 5 LOCAL VIBRATIONAL RELAXATION TIMES FOR THE STATOR PASSAGE IN FIGURE 3

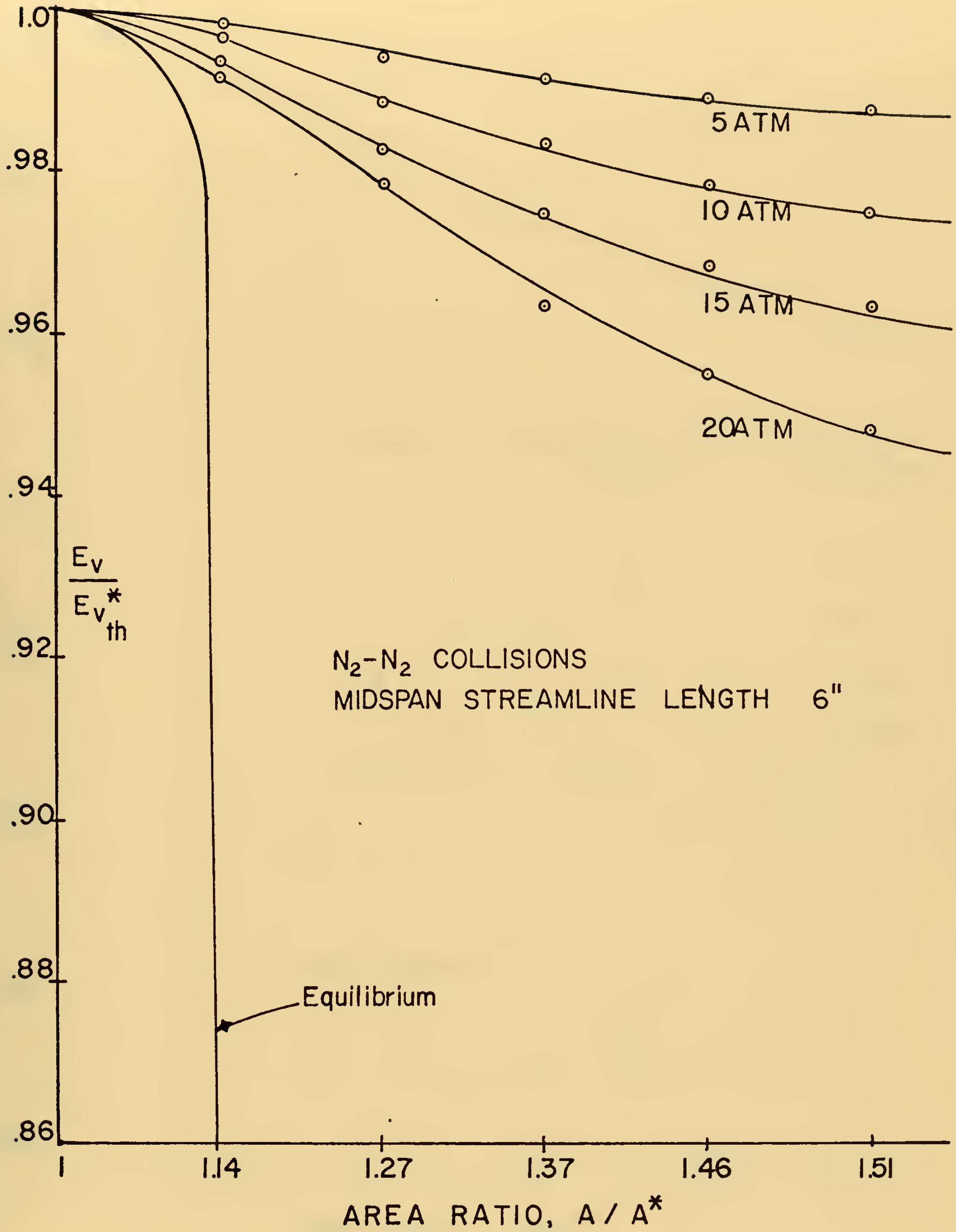

FIGURE 6 RATIO OF LOCAL VIBRATIONAL ENERGY TO EQUILIBRIUM THROAT VIBRATIONAL ENERGY AS A FUNCTION OF AREA RATIO FOR PURE NITROGEN

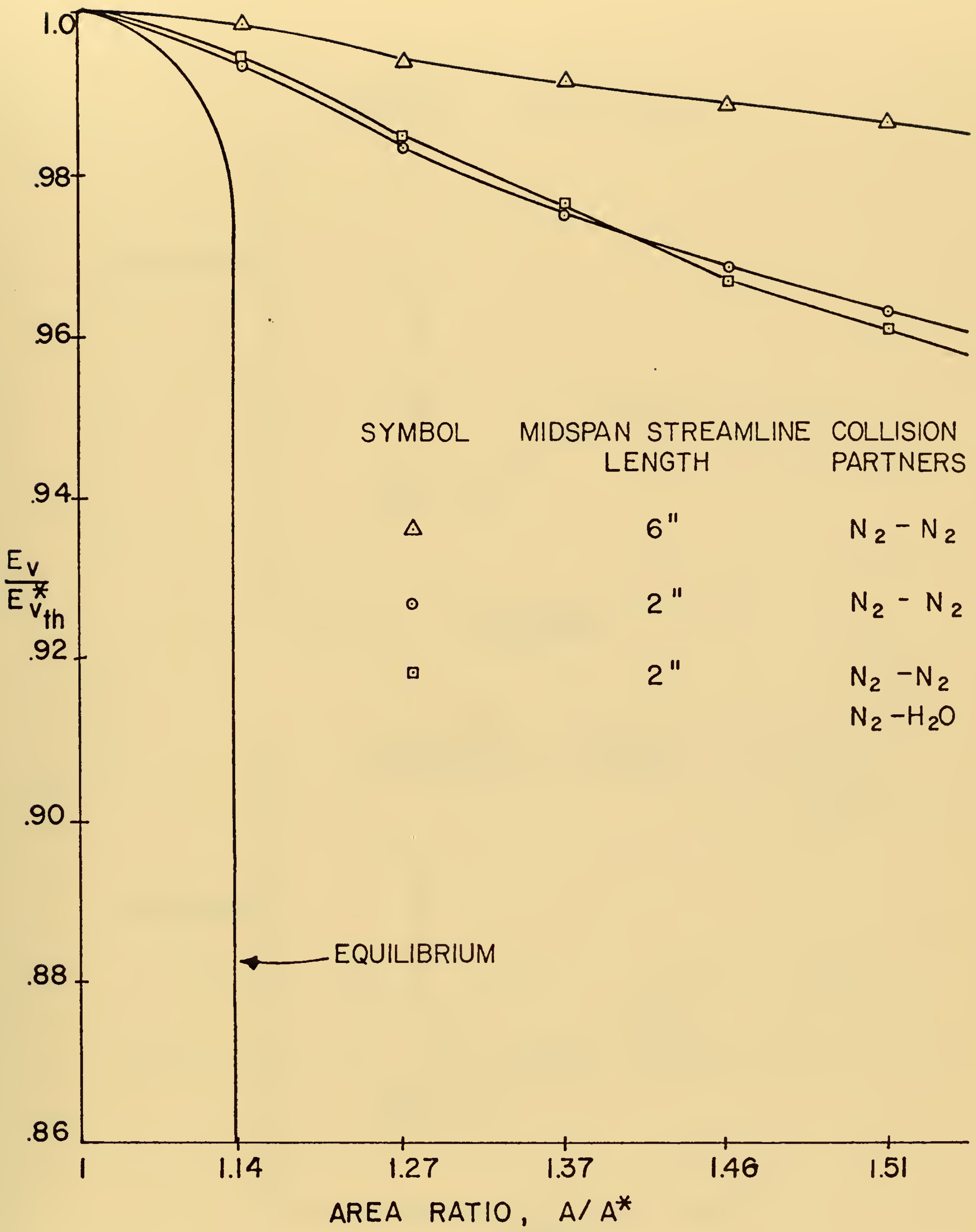

FIGURE 7 INFLUENCE OF STATOR SIZE AND COLLISION PARTNER ON THE RATIO OF LOCAL VIBRATIONAL ENERGY TO EQUILIBRIUM THROAT VIBRATIONAL ENERGY AS A FUNCTION OF AREA RATIO

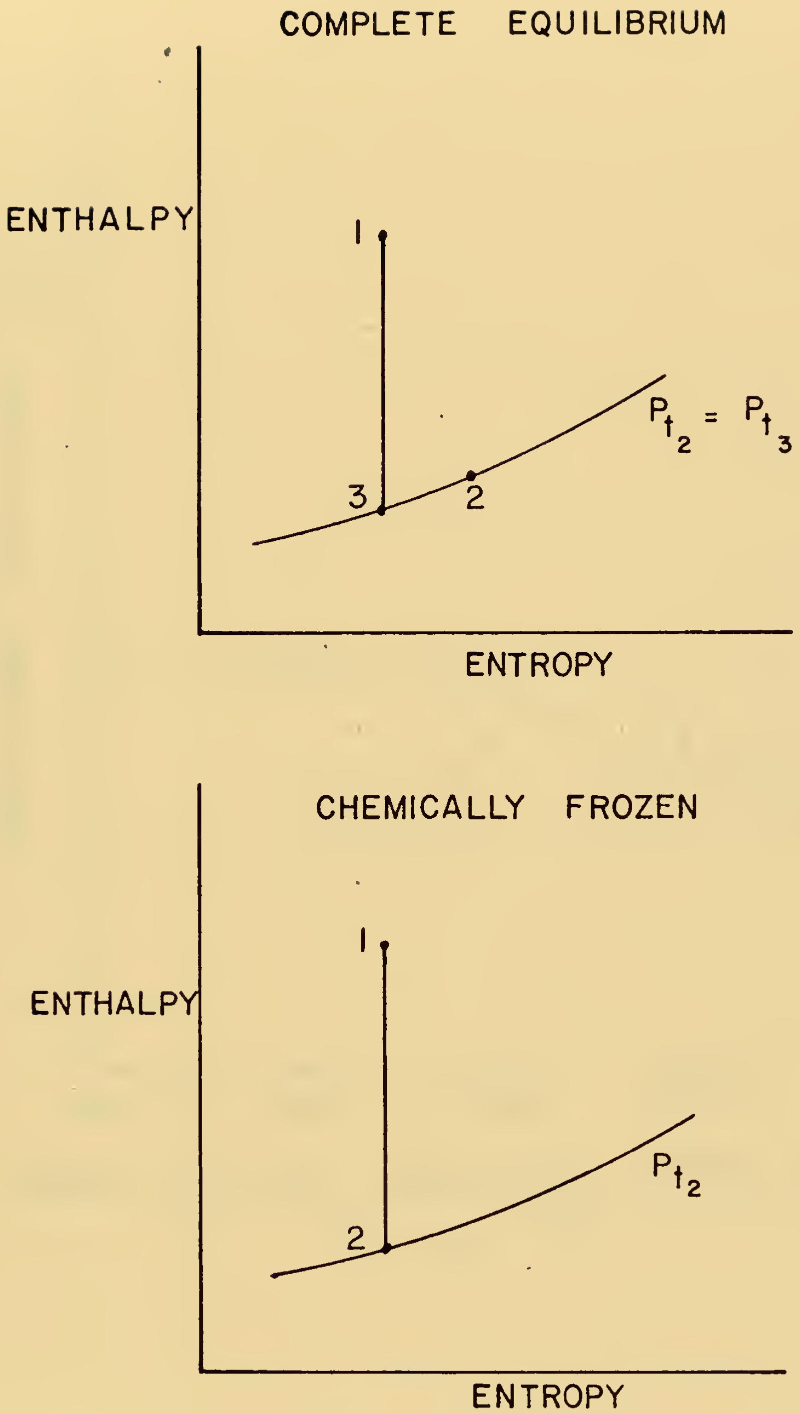

FIGURE 8 EXPANSION PROCESSES USED IN ANALYSIS OF CHEMICAL FREEZING

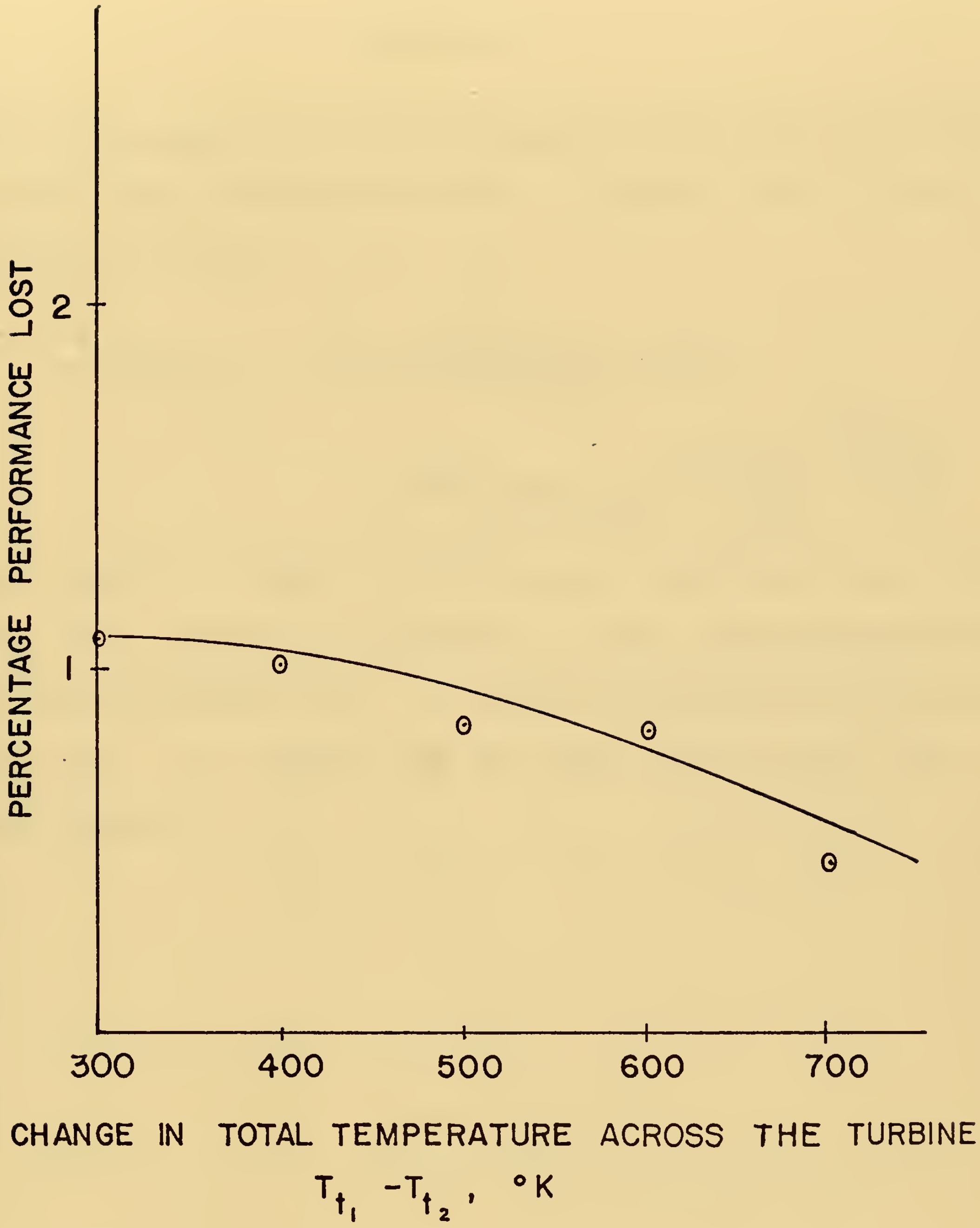

FIGURE 9 PERCENTAGE PERFORMANCE LOST AS A RESULT OF CHEMICAL FREEZING

APPENDIX C

An approximate solution to equation (21) may be obtained using the finite difference method. Equation (21) is put in the form as in Hurle, et al., [9].

$$E(T_v)_{n+1} = \frac{[1 - (\Delta x/2\lambda_n)]}{[1 + (\Delta x/2\lambda_{n+1})]} E(T_v)_n + \frac{\Delta x/2}{[1 + (\Delta x/2\lambda_{n+1})]} \frac{E(T)_{n+1}}{\lambda_{n+1}} + \frac{E(T)_n}{\lambda_n}$$

where n and n + 1 refer to two adjacent locations along the nozzle axis separated by distance Δx, and λ and T are evaluated for equilibrium flow. λ is the characteristic relaxation length and $\lambda = U\tau$, where U is the local gas velocity and τ is relaxation time.

APPENDIX D

This is the calculation of the conversion constant for use in the rate equations so that mole fractions may be utilized directly.

The units of the rate constants in Table XI vary with the type of elementary equation; bi-molecular or tri-molecular. The normal units for concentrations are moles - cm^{-3} and the units of X are moles of specie i per mole of mixture. From the ideal gas law

$$P\ V = n\ R\ T$$

Multiplying by moles of specie i over moles of specie i

$$P\ V\ X_i = n_i\ R\ T$$

or

$$\frac{n_i}{V} = \frac{P\ X_i}{R\ T}$$

in units of moles - cm^{-3}; the desired units.

Using the gas constant equal to

$$R = 82.06\ \frac{cm^3\ atm}{mole\ °K}$$

a conversion factor for use at a specified temperature and mixture pressure can be obtained. The mole fractions are each multiplied by this factor and are then ready for use in the specie rate equations.

BIBLIOGRAPHY

1. Anderson, J. D., Jr., A Time-Dependent Analysis for Quasi-One-Dimensional Nozzle Flows with Vibrational and Chemical Nonequilibrium, NOLTR 69-52, United States Naval Ordinance Laboratory, May 1969.

2. Anderson, J. D., Jr., Humphrey, R. L.; Vamos, J. S.; Plummer, M. J.; and Jenson, R. E., Population Inversions in an Expanding Gass Theory and Experiment, NOLTR 71-116, United States Naval Ordinance Laboratory, June 1971.

3. Banes, B.; McIntyre, R. W.; and Sims, J. A., Properties of Air and Combustion Products with Kerosine and Hydrogen Fuels, Bristol Siddeley Engines Limited, published on behalf of The Propulsion and Energetics Panel of the Advisory Group for Aerospace Research and Development of NATO, 1967.

4. Bray, K. N. C., Atomic Recombination in the Hypersonic Wind-Tunnel Nozzle, Journal of Fluid Mechanics, v. 6, July 1959.

5. Bray, K. N. C. and Appleton, J. P., Atomic Recombination in Nozzles: Methods of Analysis for Flows with Complicated Chemistry, A.A.S.U. Report 166, April 1964.

6. Cox, R. N. and Crabtree, L. F., Elements of Hypersonic Aerodynamics, Academic Press, 1965.

7. Erickson, W. D., Vibrational-Nonequilibrium Flow of Nitrogen in Hypersonic Nozzles, NASA TN D-1810, Langley Research Center, June, 1963.

8. Gordon, S. and Zeleznik, F. J., General IBM 704 or 7090 Computer Program for Computation of Chemical Equilibrium Composition, Rocket Performance, and Chapman-Jouguet Detonation, NASA TN D-1454, Lewis Research Center, October 1962.

9. Hurle, I. R., Russo, A. L., and Hall, J. G., Spectroscopic Studies of Vibrational Nonequilibrium in Supersonic Nozzle Flows, Journal of Chemical Physics, v. 50, No. 8, 15 April 1964, p. 2076 - 2089.

10. Newhall, H. K., Kinetics of Engine-Generated Nitrogen Oxides and Carbon Monoxide, Twelfth Symposium (International) on Compustion, p. 603.

11. Keenan, J. H. and Kaye, J., Gas Tables, John Wiley and Sons, 1945.

12. Penner, S. S., Chemical Reactions in Flow Systems, Butterworths, 1955.

13. Penner, S. S., Chemistry Problems in Jet Propulsion, Pergamon Press, 1957.

14. Pratt, G. L., Gas Kinetics, John Wiley and Sons, 1969.

15. Read, A. W., Vibrational Relaxation in Gases, Progress in Reaction Kinetics , vol. 3, Pergamon Press, 1965, p. 203-235.

16. Rich, J. W. and Treanor, C. E., Vibrational Relaxation in Gas-Dynamic Flows, Annual Review of Fluid Mechanics, vol. 2, 1970.

17. Stollery, J. L. and Park, C., Computer Solutions to the Problem of Vibrational Relaxation in Hypersonic Nozzle Flows, Imperial College of Science and Technology, Report No. 115, January 1963.

18. Taylor, R. L. and Bitterman, S., Survey of Vibrational Relaxation Data for Processes Important in the CO_2 - N_2 Laser System, Reviews of Modern Physics, v. 41, No. 1, January 1969, p. 26-45.

19. Varva, M. H., Aero-Thermodynamics and Flow in Turbomachines, John Wiley and Sons, 1960.

20. Vincenti, W. G. and Kruger, C. H., Jr., Introduction to Physical Gas Dynamics, 1965.

21. Wang, C. J., Peterson, J. B., and Anderson, R., Gas Flow Tables, GM-TR-154, Space Technology Laboratories, 14 March 1957.

22. Wilson, J. L., Schofield, D. and Lapworth, K. C., A Computer Program for Nonequilibrium Convergent-Divergent Nozzle Flow, National Physical Laboratory Report 1250, Aeronautical Research Council No. A.R.C. 29246, October 1967.

23. Zupnik, T. F., Nilson, E. N., and Sarli, V. J., Investigation of Nonequilibrium Flow Effects in High Expansion Ratio Nozzles, Computer Program Manual, NASA CR-54042, September 1964.

INITIAL DISTRIBUTION LIST

		No. Copies
1.	Defense Documentation Center Cameron Station Alexandria, Virginia 22314	2
2.	Library, Code 0212 Naval Postgraduate School Monterey, California 93940	2
3.	Professor R. W. Bell, Code 57 Be Chairman, Department of Aeronautics Naval Postgraduate School Monterey, California 93940	1
4.	Professor A. E. Fuhs, Code 57 Fu Department of Aeronautics Naval Postgraduate School Monterey, California 93940	10
5.	LCDR Wiley P. DeCarli, USN 444 Dela Vina Ave D-1 Monterey, California 93940	1
6.	Professor D. W. Netzer, Code 57 Nt Department of Aeronautics Naval Postgraduate School Monterey, California 93940	1
7.	Mr. Eric Lister Research and Technology Division Naval Air Propulsion Test Center Trenton, New Jersey 08628	1
8.	Mr. Frank R. Johns Systems Analysis and Engineering Department Naval Air Development Center Warminster, Pennsylvania 18974	1
9.	Dr. Robert Oliver Institute for Defense Analysis 400 Army Navy Drive Arlington, Virginia 22202	1

		No. Copies
10.	Mr. Raymond M. Standahar DDR&E (Room 3E 1047) Pentagon Washington, D.C. 20301	1
11.	Mr. Robert Brown (NAVAIR 536B2) Naval Air Systems Command Washington, D.C. 20360	1
12.	Dr. William Heiser Chief Scientist AFAPL Wright-Patterson AFB, Ohio 45433	1
13.	Dr. D. Zonars Chief Scientist AFFDL Wright-Patterson AFB, Ohio 45433	1
14.	Dr. Hans Von Ohain Chief Scientist ARL Wright-Patterson AFB, Ohio 45433	1
15.	Mr. Clifford Simpson Chief, Turbine Engine Division AFAPL Wright-Patterson AFB, Ohio 45433	1
16.	Dr. R. E. Henderson Detroit Diesel Allison Division of GMC P.O. Box 894 Indianapolis, Indiana 46206	1
17.	Mr. Calvin Emerson Detroit Diesel Allison Division P.O. Box 894 Indianapolis, Indiana 46206	1
18.	Mr. James Byers, Code (536) Naval Air Systems Command Washington, D.C. 20360	1
19.	Professor Forman A. Williams University of California, San Diego LaJolla, California 92037	1
20.	Dr. Marshall Lapp General Electric Research and Development Center P.O. Box 8 Schenectady, New York 12301	1

		No. Copies
21.	Dr. J. D. Anderson Naval Ordnance Laboratory Silver Springs, Maryland 20910	1
22.	Dr. D. L. Harshman High Temperature Technology - Large Engines General Electric Aircraft Engines Evendale, Ohio 45240	1
23.	Mr. Harold D. Altis Director, Advanced Engineering McDonnell-Douglas Aircraft Company Saint Louis, Missouri 63166	1
24.	Mr. John White Eustis Directorate SAVDL USAAMRDL Fort Eustis, Virginia 23604	1
25.	Dr. Michael Suo Manager, Turbine Research and Development Pratt and Whitney Aircraft 400 Main Street East Hartford, Connecticut 06108	1
26.	Mr. Donald Dahlberg Manager, Turbine Research and Development Pratt and Whitney Aircraft Florida Research and Development Center West Palm Beach, Florida 33401	1
27.	Dr. Herbert Mueller, Code 310 Naval Air Systems Command Washington, D.C. 20360	1
28.	Mr. William Zazaky Pratt and Whitney Aircraft 400 Main Street East Hartford, Connecticut 06108	1

DOCUMENT CONTROL DATA - R & D

(Security classification of title, body of abstract and indexing annotation must be entered when the overall report is classified)

1. ORIGINATING ACTIVITY *(Corporate author)*
Naval Postgraduate School
Monterey, California 93940

2a. REPORT SECURITY CLASSIFICATION
Unclassified

2b. GROUP

3. REPORT TITLE
VIBRATIONAL AND CHEMICAL NONEQUILIBRIUM
IN A STOICHIOMETRIC TURBOJET ENGINE
USING KEROSINE-TYPE FUEL

4. DESCRIPTIVE NOTES *(Type of report and, inclusive dates)*
Master's Thesis (March 1972

5. AUTHOR(S) *(First name, middle initial, last name)*
Wiley Paul DeCarli
Lieutenant Commander, United States Navy

6. REPORT DATE
March 1972

7a. TOTAL NO. OF PAGES
76

7b. NO. OF REFS
23

8a. CONTRACT OR GRANT NO.

b. PROJECT NO.

c.

d.

9a. ORIGINATOR'S REPORT NUMBER(S)

9b. OTHER REPORT NO(S) *(Any other numbers that may be assigned this report)*

10. DISTRIBUTION STATEMENT
Approved for public release; distribution unlimited.

11. SUPPLEMENTARY NOTES

12. SPONSORING MILITARY ACTIVITY
Naval Postgraduate School
Monterey, California 93940

13. ABSTRACT

The effects of vibrational and chemical nonequilibrium on turbine performance were investigated separately. The vibrational model was taken as a pure nitrogen expansion, and the chemical model was taken as the combustion products of a stoichiometric mixture of kerosene and air. The loss of performance of fully frozen flow with respect to the equilibrium flow for each model was determined. The extent to which nonequilibrium will occur was investigated within limited ranges of pressure and temperature. Vibrational nonequilibrium can result in losses up to seven percent with respect to equilibrium flow. Vibrational freezing will be virtually complete a short distance after the throat of the first stator assembly. The losses due to chemical nonequilibrium are insignificant compared to the vibrational nonequilibrium losses.

KEY WORDS	LINK A		LINK B		LINK C	
	ROLE	WT	ROLE	WT	ROLE	WT
Stoichiometric Turbojet Vibrational Nonequilibrium Chemical Nonequilibrium						

DeCarli

Vibrational and chemical nonequilibrium in a stoichiometric turbojet engine using kerosine-type fuel.

Thesis 133853
D2
c.1

DeCarli

Vibrational and chemical nonequilibrium in a stoichiometric turbojet engine using kerosine-type fuel.